

---

## CHAPTER - 3

### **ELECTROMAGNETIC MODE ANALYSIS OF PLANAR OPTICAL WAVEGUIDE WITH NEARLY PARABOLIC REFRACTIVE INDEX PROFILE**

---

### 3.1 Introduction :

In the earlier chapter we have briefly described the electromagnetic mode treatment of planar waveguides consisting of materials with parabolic index profile. Such waveguides play a vital role in many integrated optical devices. However the parabolic index variation is disadvantageous in two ways : i) It is applicable to symmetric waveguides only. ii) It does not include cladding effects, particularly the behaviour of modes near cut-offs. Apart from these profiles there are a number of refractive index profiles associated with the planar waveguides used in integrated optics. The exact solutions of the scalar wave equation for both TE and TM modes have been reported in the literature for such refractive index profiles<sup>1-3</sup>.

The manufacturing problems cause distortions in the shapes of the desired refractive index profiles. For instance, the most probable deviation introduced in a true parabolic profile is of flat continuation nature<sup>4-6</sup>. In the present chapter we consider a symmetric planar waveguide with such a refractive index profile and work out the detailed modal analysis.

### 3.2 Electromagnetic Mode Analysis of Inhomogeneous Optical Waveguides : (Present Work)

#### Expression for Nearly Parabolic Refractive Index Profile<sup>6</sup> :

We consider a planar symmetric optical waveguide having a parabolic refractive index profile with flat

continuation in the guiding layer. For the flat region  $0 \leq x \leq a$ ,  $n^2(x) = n_1^2$  while in the region  $a \leq x \leq \rho$ , the refractive index distribution is defined as

$$n^2(x) = \left[ n_1^2 (x^2 - \rho^2) - n_2^2 (x^2 - a^2) \right] / (a^2 - \rho^2) \quad \dots\dots (3.1)$$

where  $\rho$  = width of guiding layer,  $n_2$  = refractive index of substrate/superstrate, while the flat continuation is characterised by the width 'a' and refractive index  $n_1$ . It is to be noted that for  $x = a$  and  $\rho$ , Eq.(3.1) gives the refractive indices  $n_1$  and  $n_2$  respectively; while for  $a = 0$ , it represents the true parabolic refractive index profile which has been discussed already in Sec.(2.4).

Eq.(3.1) can be simplified as follows :

$$n^2(x) = \frac{n_1^2(\rho^2 - x^2)}{(\rho^2 - a^2)} + \frac{n_2^2(x^2 - a^2)}{(\rho^2 - a^2)}$$

By adding and subtracting  $a^2$  in the numerator of first term and simplifying we get

$$n^2(x) = \bar{n}_1^2 - \left[ \frac{\rho^2}{(\rho^2 - a^2)} (n_1^2 - n_2^2) \right] \left( \frac{x}{\rho} \right)^2$$

with  $\bar{n}_1^2 = n_1^2 + a^2 2\Delta n_1^2 a_1^2 / (1 - a_1^2) \quad \dots\dots (3.2)$

where  $a_1 = a / \rho$

The bracket in the second term of above equation is simplified by adding and subtracting  $n_2^2$ .

$$n^2(x) = \bar{n}_1^2 - (\bar{n}_1^2 - n_2^2) x_1^2 \quad \dots\dots (3.3)$$

with  $x_1 = x / \rho$ .

Eq.(3.3) can be rewritten as

$$n^2(x) = \bar{n}_1^2 (1 - 2\bar{\Delta} x_1^2) \quad \dots\dots (3.4)$$

where  $2\bar{\Delta} = 1 - n_2^2 / \bar{n}_1^2$

which can be simplified using Eq.(3.2)

$$2\bar{\Delta} = \frac{2\Delta}{1 + a_1^2(2\Delta - 1)} \quad \dots\dots (3.5)$$

where  $2\Delta \approx (n_1 - n_2) / n_1$  and  $a_1 = a / \rho$  is a measure of 'relative distortion' in the parabolic refractive index profile.

The final form of Eq.(3.4) is given as

$$n^2(x) = \bar{n}_1^2 - \bar{n}_2^2 x_1^2 \quad \dots\dots (3.6)$$

with  $\bar{n}_2^2 = 2\bar{\Delta} \bar{n}_1^2$

Using Eq.(3.6) the distorted parabolic refractive index profile can be plotted graphically. Typical profiles for relative distortions 0.3 and 0.7 are shown in Fig.(3.1). In view of the fact that Eq.(3.1) holds good in the range  $a \leq x \leq \rho$ , the Eqs.(3.2) and (3.5) are valid for the relative distortion in the range  $0 \leq a_1 < 1$ .

### Electromagnetic Mode Treatment :<sup>1,7,11</sup>

We carry out the analysis by adopting the procedure outlined in Sec.(2.4.1) and obtain both TE and TM solutions for the scalar wave equation which involves the distribution of refractive index given by Eq.(3.6).

#### 3.2.1 TE solutions :

Using Eqs.(3.2)-(3.6) we rewrite Eq.(2.20)

$$\frac{d^2 H_x}{dx^2} + \left[ k^2 \bar{n}_1^2 (1 - 2\bar{\Delta} x_1^2) - \beta^2 \right] H_x = 0 \quad \dots\dots (3.7)$$

We assume the following trial solution.

$$H_x(x) = X(x) \exp(-x^2 / w_a^2) \quad \dots\dots (3.8)$$

Hence Eq. (3.7) becomes

$$\frac{d^2X}{dx^2} - \frac{4x}{w_1^2} \frac{dX}{dx} - \frac{2}{w_1^2} \left(1 - \frac{2x^2}{w_1^2}\right) X + \left[ k^2 \bar{n}_1^2 (1 - 2\bar{\Delta} x_1^2) - \beta^2 \right] X = 0 \quad \dots (3.9)$$

We now define an "effective beam-waist" as follows

$$w_1^2 = \frac{2\rho}{k\bar{n}_1 (2\bar{\Delta})^{1/2}} \quad \dots (3.10)$$

Using the definitions of  $\bar{n}_1$  and  $2\bar{\Delta}$  as given in Sec. (3.1.1)

we can simplify Eq. (3.10) as

$$w_1^2 = w_0^2 (1 - a_1^2)^{1/2} \quad \dots (3.11)$$

where  $w_0$  is the usual beam-waist given by Eq. (2.24). It is to be noted that  $w_1$  depends upon the relative distortion associated with the refractive index profile. It decreases with increase in distortion. However it becomes invalid as  $a_1 \rightarrow 1$ .

Eq. (3.9) can be converted into the familiar form of Hermite differential equation by employing the transformation  $x' = x \sqrt{2} / w_1$  and the resulting expressions therefrom.

$$\frac{dX}{dx} = \frac{\sqrt{2}}{w_1} \frac{dX}{dx'}, \quad \frac{d^2X}{dx^2} = \frac{2}{w_1^2} \frac{d^2X}{dx'^2}$$

and 
$$\bar{\Delta} (k \bar{n}_1 x_1 w_1)^2 = x'^2$$

Thus Eq. (3.9) takes the form

$$\frac{d^2X}{dx'^2} - 2x' \frac{dX}{dx'} + \left[ (k^2 \bar{n}_1^2 - \beta^2) \frac{w_1^2}{2} - 1 \right] X = 0 \quad \dots (3.12)$$

The solutions<sup>11</sup> of this equation would be Hermite-polynomials  $H_N(x')$  for which  $N$  and  $\beta$  are related through

$$2N = (k^2 \bar{n}_1^2 - \beta^2) \frac{w_1^2}{2} - 1 \quad \dots\dots (3.13)$$

with  $N = 0, 1, 2, \dots$

Using  $H_N(x')$  in Eq.(3.8) the solution for the TE modes is written as

$$H_x = \frac{(2/\pi)^{1/4}}{(2^N N! w_1)^{1/2}} H_N \left[ \frac{x\sqrt{2}}{w_1} \right] \exp(-x^2/w_1^2) \quad \dots (3.14)$$

The multiplying constant is chosen so as to satisfy the normalisation condition, namely

$$\int_{-\infty}^{\infty} |H_x|^2 dx = 1$$

$\bar{b} - v$  curves :

Eq.(3.13) is the eigenvalue equation for TE modes. We define the following effective normalised variables in terms of relative distortion  $a_1$ .

$$\begin{aligned} \bar{u}^2 &= \rho^2 (k^2 \bar{n}_1^2 - \beta^2) \\ \bar{v}^2 &= \frac{v^2}{(1 - a_1^2)} \end{aligned} \quad \dots\dots (3.15)$$

Using these in Eq.(3.11) alongwith Eq.(2.24) we get

$$w_1^2 = 2\rho^2 / \bar{v} \quad \dots\dots (3.16)$$

Hence Eq.(3.13) is converted into the form

$$2N = \bar{u}^2 / \bar{v} - 1 \quad \text{or} \quad \bar{u}^2 = (2N + 1) \bar{v} \quad \dots\dots (3.17)$$

The effective normalised propagation constant is then given by

$$\bar{b} = 1 - (\bar{u} / \bar{v})^2 = 1 - (2N + 1) / \bar{v} \quad \dots\dots (3.18)$$

This expression is useful for plotting  $\bar{b} - v$  curves for various  $TE_N$  modes in the presence of different relative distortions. It is to be noted that at  $\bar{b} = 0$  we have

$$\bar{v}_0 = (2N + 1) \quad \text{or} \quad v_0 = (1 - a_1^2)^{1/2} (2N + 1) \quad \dots (3.19)$$

Thus in the present work the cut-off frequency for a given mode is seen to be reduced by a factor of  $(1 - a_1^2)^{1/2}$ .

Group Delay<sup>10</sup> : From Eq.(3.13) we can obtain

$$\beta^2 = k^2 \bar{n}_1^2 - (2/w_1^2)(2N + 1) \quad \dots\dots (3.20)$$

This can be further simplified with the help of Eqs.(3.2) and (3.11).

$$\beta^2 = k^2 n_1^2 \left\{ 1 + \left[ \frac{2\Delta}{1 - a_1^2} \right]^{1/2} \left[ \frac{a_1^2}{(1 - a_1^2)^{1/2}} - \frac{(2N + 1)}{\rho k n_1} \right] \right\}$$

By taking the square root and expanding the bracketted expression binomially in ascending powers of  $\Delta^{1/2}$ , we can deduce the expression

$$\beta = \left[ 1 + \frac{(2\Delta)^{1/2} a_1^2}{2(1 - a_1^2)} \right] kn_1 - \frac{(2\Delta)^{1/2}}{\rho} (N + \frac{1}{2}) \left[ \frac{2a_1^2(2 + \Delta^{1/2})}{2(1 - a_1^2)^{3/2}} \right] - \frac{\Delta}{\rho^2 kn_1} \frac{(N + \frac{1}{2})^2}{(1 - a_1^2)} \quad \dots\dots (3.21)$$

In obtaining this expression we have neglected the terms containing  $\Delta^{3/2}$  and higher powers of  $\Delta$ .

The Group delay is given by

$$\tau_g = \frac{L}{c} \frac{d\beta}{dk}$$

So differentiating Eq.(3.21) we can obtain the group delay per unit length as

$$\frac{\tau_g}{L} = \frac{n_1}{c} \left[ 1 + \frac{(2\Delta)^{1/2} a_1^2}{2(1 - a_1^2)} + \frac{\Delta}{\rho^2 k^2 n_1^2} \frac{(N + \frac{1}{2})^2}{(1 - a_1^2)} \right] \quad \dots\dots (3.22)$$

It is interesting to note that by putting  $a_1 = 0$  in the above derived expressions we can easily deduce the

relevant expressions for true parabolic index media (Sec.2.4.1).

### 3.2.2 TM solutions :

In this case we employ the scalar wave Eq.(2.19) alongwith the Eq.(3.6) for refractive index profile. The bracketted expression in Eq.(2.19) is simplified by expanding terms in  $n^2(x)$  as a power series and neglecting terms of  $\Delta^2 x_1^4$  and higher order. The Eq.(2.19) is then written as :

$$\frac{d^2 \psi}{dx^2} + \left[ \left( k^2 \bar{n}_1^2 - \beta^2 - \frac{2\bar{\Delta}}{\rho^2} \right) - \left( \frac{k^2 \bar{n}_1^2 2\bar{\Delta}}{\rho^2} + \frac{16\bar{\Delta}^2}{\rho^4} \right) x^2 \right] \psi = 0 \quad \dots (3.23)$$

This equation has the same form as that of Eq.(3.7). By analogy with Eq.(3.8) we try the solution as below.

$$\psi(x) = X(x) \exp(-x^2 / w_2^2) \quad \dots (3.24)$$

Using Eq.(3.24) in Eq.(3.23) we can easily obtain the following equation.

$$\frac{d^2 X}{dx^2} - \frac{4x}{w_2^2} \frac{dX}{dx} - \frac{2}{w_2^2} X + \left[ k^2 \bar{n}_1^2 - \beta^2 - \frac{2\bar{\Delta}}{\rho^2} \right] X = 0 \quad \dots (3.25)$$

For the TM case we define an effective beam-waist as follows.

$$w_2^2 = 2 / \left\{ \frac{k^2 \bar{n}_1^2 2\bar{\Delta}}{\rho^2} + \frac{16\bar{\Delta}^2}{\rho^4} \right\}^{1/2} \quad \dots (3.26)$$

Utilising the expressions for  $\bar{n}_1^2$  and  $2\bar{\Delta}$  alongwith Eq.(2.34) for a normal beam-waist  $w_0$ , we can simplify Eq.(3.26).

Thus

$$\left\{ \frac{k^2 \bar{n}_1^2 2\bar{\Delta}}{\rho^2} + \frac{16\bar{\Delta}^2}{\rho^4} \right\}^{1/2} = \left\{ \frac{k^2 n_1^2 2\Delta}{\rho^2} (1 + a_1^2)^{-1} + \frac{16\Delta^2}{\rho^4} \left[ 1 - (1 - 2\Delta) a_1^2 \right]^{-2} \right\}^{1/2}$$

The bracketted expression in both the terms are then binomially expanded in the ascending powers of  $a_1^2$ . After neglecting  $a_1^4$  and higher order terms and simplifying we obtain

$$\begin{aligned} \left\{ \dots \right\}^{1/2} &= \left\{ \left[ \frac{k^2 n_1^2 2\Delta}{\rho^2} + \frac{16\Delta^2}{\rho^4} \right] + a_1^2 \left[ \left[ \frac{k^2 n_1^2 2\Delta}{\rho^2} + \frac{16\Delta^2}{\rho^4} \right] + \frac{16\Delta^2}{\rho^4} \right] \right\}^{1/2} \\ &= \left\{ \frac{4}{w_0^4} + a_1^2 \frac{4}{w_0^4} + \frac{16\Delta^2}{\rho^4} a_1^2 \right\}^{1/2} \end{aligned}$$

Putting this in Eq.(3.26) and simplifying further we get

$$w_2^2 = w_0^2 / \left\{ 1 + a_1^2 \left[ 1 + \frac{4\Delta^2 w_0^4}{\rho^4} \right] \right\}^{1/2} \quad \dots (3.27)$$

In order to convert Eq.(3.25) in the form of Hermite differential equation we adopt the transformation  $x' = x \sqrt{Z} / w_2$  and the subsequent derivatives obtained from it. Thus Eq.(3.25) becomes

$$\frac{d^2 X}{dx'^2} - 2x' \frac{dX}{dx'} + \left[ (k^2 \bar{n}_1^2 - \beta^2 - \frac{2\bar{\Delta}}{\rho^2}) \frac{w_2^2}{2} - 1 \right] X = 0$$

..... (3.28)

The solutions of this equation are nothing but the Hermite polynomials  $H_N(x')$  for which the eigenvalue equation is given as

$$2N = \left( k^2 \bar{n}_1^2 - \beta^2 - \frac{2\bar{\Delta}}{\rho^2} \right) \frac{w_2^2}{2} - 1 \quad \dots\dots (3.29)$$

with  $N = 0, 1, 2, \dots$

Using  $H_N(x')$  in Eq.(3.24) alongwith Eq.(2.18a) the solution for the TM modes is written as<sup>p</sup>

$$E_x = \frac{\psi}{n(x)} = \frac{(2/\pi)^{1/4}}{n(x)(2^N N! w_2)^{1/2}} H_N \left[ \frac{x\sqrt{2}}{w_2} \right] \exp(-x^2/w_2^2) \quad \dots\dots (3.30)$$

In this equation a normalisation constant has been appropriately chosen.

$\bar{b} - v$  curves :

The eigenvalue Eq.(3.29) can be expressed in terms of normalised variables and propagation constant as explained below.

We define the following effective normalised variables.

$$\bar{u}^2 = \rho^2 (k^2 \bar{n}_1^2 - \beta^2) \quad \dots\dots (3.31a)$$

Eq.(3.26) is rewritten as

$$w_2^2 = 2\rho^2 / \left[ \rho^2 k^2 \bar{n}_1^2 2\bar{\Delta} + 16\bar{\Delta}^2 \right]^{1/2}$$

Comparing this with Eq.(2.34) we can define an effective normalised frequency for the TM modes as below.

$$\bar{v} = \left[ \rho^2 k^2 \bar{n}_1^2 2\bar{\Delta} + 16\bar{\Delta}^2 \right]^{1/2}$$

which upon simplification takes the form

$$\bar{v} = \left[ \frac{v^2}{(1 - a_1^2)} + \frac{16\bar{\Delta}^2}{\left[ (1 - a_1^2) + 2\Delta a_1^2 \right]^2} \right]^{1/2} \quad \dots\dots (3.31b)$$

$$w_2^2 = 2\rho^2 / \bar{v} \quad \dots\dots (3.31c)$$

Using the above expressions we can simplify the eigenvalue Eq.(3.29) as

$$2N = \frac{\bar{u}^2}{\bar{v}} - \frac{2\Delta}{\left[(1 - a_1^2) + 2\Delta a_1^2\right]\bar{v}} - 1$$

or

$$\bar{u}^2 = (2N + 1)\bar{v} + \frac{2\Delta}{\left[(1 - a_1^2) + 2\Delta a_1^2\right]} \quad \dots (3.31d)$$

Hence the effective normalised propagation constant is given by

$$\bar{b} = 1 - \frac{\bar{u}^2}{\bar{v}^2}$$

i.e.  $\bar{b} = 1 - \frac{(2N + 1)}{\bar{v}} - \frac{2\bar{\Delta}}{\bar{v}^2} \quad \dots (3.32)$

This expression can be employed to calculate  $\bar{b} - v$  curves in the case of  $TM_N$  modes by taking into account different relative distortions in the parabolic refractive index profile.

For  $\bar{b} = 0$  we obtain the following cut-off frequency condition.

$$\bar{v}_c^2 - \bar{v}_c(2N + 1) - 2\bar{\Delta} = 0$$

Solving the quadratic equation we get

$$\bar{v}_c = \frac{(2N + 1) \pm \sqrt{(2N + 1)^2 + 8\bar{\Delta}}}{2} \quad \dots (3.33)$$

Group Delay<sup>10</sup> : Eq.(3.29) can be rewritten as

$$\beta^2 = k^2 \bar{n}_1^2 - \frac{2\bar{\Delta}}{\rho^2} - (2/w_2^2)(2N + 1) \quad \dots (3.34)$$

Employing the definitions of  $\bar{n}_1^2$ ,  $2\bar{\Delta}$  and  $w_2^2$  we can simplify different terms in the above equation as below

$$\frac{2}{w_2^2} = \frac{kn_1 (2\Delta)^{1/2}}{\rho} \left\{ 1 + \frac{8\Delta}{\rho^2 k^2 n_1^2} \right\}^{1/2} \left\{ 1 + a_1^2 \left[ 1 + \frac{4\Delta^2 w_0^4}{\rho^4} \right] \right\}^{1/2}$$

Expanding the bracketted expressions binomially and neglecting  $\Delta^3$  and higher order terms we obtain

$$\frac{2}{w_2^2} \approx \frac{kn_1 (2\Delta)^{1/2}}{\rho} \left\{ 1 + \frac{4\Delta}{\rho^2 k^2 n_1^2} + \frac{a_1^2}{2} + \frac{2\Delta a_1^2}{\rho^2 k^2 n_1^2} \right\}$$

Similarly we get

$$\frac{2\bar{\Delta}}{\rho^2} \approx \frac{2\Delta}{\rho^2} \left[ 1 - a_1^2 (2\Delta - 1) \right]$$

In this case we have neglected  $a_1^3$  and higher order terms. Using these alongwith Eq.(3.2) we further simplify Eq.(3.34) to deduce

$$\beta^2 \approx k^2 n_1^2 \left\{ 1 - 2\Delta \left[ p + q(2\Delta)^{1/2} \right] \right\}$$

where

$$p = \frac{(1 + a_1^2 / 2)(2N + 1)}{\rho kn_1} \quad \text{and}$$

$$q = \left[ \frac{1 - a_1^2}{\rho^2 k^2 n_1^2} - \frac{a_1^2}{1 - a_1^2} \right]$$

By taking the square root and expanding binomially in the ascending powers of  $(2\Delta)^{1/2}$ , we get finally the expression for  $\beta$  as below

$$\begin{aligned} \beta \approx kn_1 - \frac{(2\Delta)^{1/2}}{\rho} \left( 1 + \frac{a_1^2}{2} \right) \left( N + \frac{1}{2} \right) \\ - \frac{\Delta}{\rho^2 kn_1} \left[ \left( 1 + \frac{a_1^2}{2} \right)^2 \left( N + \frac{1}{2} \right)^2 + (1 + a_1^2) - \left( \frac{a_1^2}{1 - a_1^2} \right) \rho^2 k^2 n_1^2 \right] \\ \dots\dots (3.35) \end{aligned}$$

The group delay is defined as

$$\tau_g = \frac{L}{c} \frac{d\beta}{dk}$$

Differentiating Eq.(3.35) with respect to  $k$  we can deduce the group delay per unit length as follows

$$\frac{\tau_g}{L} = \frac{n_1}{c} \left\{ 1 + \left[ \frac{a_1^2}{1 - a_1^2} \right] \Delta + \frac{\Delta}{\rho^2 k^2 n_1^2} \left[ \left( 1 + \frac{a_1^2}{2} \right) \left( N + \frac{1}{2} \right)^2 + a_1^2 + 1 \right] \right\} \dots\dots (3.36)$$

It is to be noted that by substituting  $a_1 = 0$  in all the above derived expressions one can easily obtain the relevant expressions for TM mode in true parabolic index media (Sec.2.4.1).

For small  $\Delta/\rho^2 k^2 n_1^2$  and  $a_1^2$  we note that Eq.(3.36) is approximated to

$$\frac{\tau_g}{L} \approx \frac{n_1}{c} \left\{ 1 + \left[ \frac{a_1^2}{1 - a_1^2} \right] \Delta + \frac{\Delta}{\rho^2 k^2 n_1^2} \left( N + \frac{1}{2} \right)^2 \left( 1 + \frac{a_1^2}{2} \right) \right\} \dots\dots (3.37)$$

Similarly Eq.(3.22) becomes

$$\frac{\tau_g}{L} \approx \frac{n_1}{c} \left\{ 1 + \left[ \frac{a_1^2}{1 - a_1^2} \right] \frac{(2\Delta)^{1/2}}{2} + \frac{\Delta}{\rho^2 k^2 n_1^2} \left( N + \frac{1}{2} \right)^2 \left( 1 + a_1^2 \right) \right\} \dots\dots (3.38)$$

From the above simplified expressions we note that for a given relative distortion  $a_1$  and for small  $\Delta/\rho^2 k^2 n_1^2$

- i) the group delay per unit length is approximately the same for TE and TM modes (except for few low-order modes).
- ii) the TE and TM modes are quasi-degenerate.
- iii) the group delay per unit length is almost the same for all modes.

### 3.2.3 Radiation Confinement Factor (TE/TM degeneracy) :

By taking into account the TE/TM degeneracy in the limit of small  $\Delta$  we write expressions for the radiation confinement factor in analogy with Eqs.(2.41).

$$N = 0 : \Gamma_0 = 1 - \frac{2}{\sqrt{\pi}} \frac{e^{-\bar{v}}}{2\bar{v}^{-1/2}} \left[ 1 - \frac{1}{2\bar{v}} + \frac{3}{4\bar{v}^2} - \frac{15}{8\bar{v}^3} + \dots \right] \quad \dots\dots (3.39)$$

$$N = 1 : \Gamma_1 = \Gamma_0 - \frac{2\bar{v}^{-1/2}}{\pi^{1/2}} e^{-\bar{v}} \quad \dots\dots (3.40)$$

with  $\bar{v} = \frac{v}{(1 - a_1^2)^{1/2}}$  for TE case.

## 3.3 Results and Discussion :

### 3.3.1 TE Case :

#### a) H<sub>x</sub> Field distributions :

In order to calculate field distributions for TE<sub>N</sub> modes we have made use of Eq.(3.14) alongwith Eq.(3.11) for the effective beam-waist. The field values have been calculated by varying the relative distortion  $a_1$  between 0 and 0.9 by regular steps. The calculated results are presented in two ways. In tabular form are given the calculated field distributions for TE<sub>0</sub>, TE<sub>1</sub>, TE<sub>2</sub> and TE<sub>3</sub> modes by taking even values for  $a_1$  (Tables 3.1 and 3.2). Graphically the results are illustrated again in two ways. In Fig.(3.2) we find field distributions for TE<sub>0</sub> and TE<sub>1</sub> modes by taking odd values (including 0) for  $a_1$ . In Figs.(3.4) and (3.5) we have given comparative field distributions of first four TE modes for given distortion level.

From Tables (3.1) and (3.2) and Figs.(3.2) and (3.3) we note the following observations :

i) For  $N = 0$  mode and given  $a_1$  value, the field  $H_x$  increases in the beginning and after reaching a peak value drops down to zero. Further with increase of distortion level the peak value of  $H_x$  goes on increasing regularly. This is clearly seen in Fig.(3.2) for  $TE_0$  mode. We also note from this figure that with the increase in distortion the extent of field distribution of a given mode reduces. This suggest more confinement of power near the axis due to increase in distortion. For  $a_1 = 0$  we get the field distribution of  $TE_0$  mode for a true parabolic index medium which has the lowest peak value.

ii) For  $N = 1, 2,$  and  $3$  modes and for a given  $a_1$  value, it is seen that the field distributions are oscillatory in nature with different number of minima and maxima. With the increase in distortion for these modes it is found that the minimum of  $H_x$  shifts towards negative values while maximum of  $H_x$  increases. For all the three modes the spread of field patterns decreases due to increase in distortion level. This favours again for confinement of power of a given mode near the axis of the waveguide.

From Figs.(3.4) and (3.5) we note that for a given distortion the maxima and minima decrease as the mode order increases. Further the decrease in the extent of field patterns due to increase in distortion is clearly seen from the two figures.

b)  $\bar{b} - v$  curves :

We have used Eq.(3.18) alongwith the definition of  $\bar{v}$  and have calculated  $\bar{b} - v$  curves for the first four  $TE_N$  modes by considering the distortion effect. The calculated results are presented both in tabular form (Tables 3.3 and 3.4) and graphically (Figs. 3.6 and 3.7).

From the above mentioned tables and figures we note the following facts.

i) For a given TE mode, the cut-off frequency shifts towards zero with increase in distortion level in the parabolic refractive index profile.

ii) For a given distortion, the cut-off frequency increases with the increase in mode order. This behaviour is in agreement with the universal character of  $b - v$  curves for any given medium.

iii) For a given TE mode the asymptotic part of  $\bar{b} - v$  curves shifts towards unity with the increase in distortion level.

3.3.2 TM Case :

a)  $E_x$  Field Distributions :

The  $E_x$  field distributions have been calculated using Eqs.(3.30) and (3.27) and the results are illustrated both in tabular form (Tables 3.5 and 3.6) and graphically (Fig. 3.10-3.13). We note the following findings from the calculated results.

i) For  $N = 0$  mode and given distortion value, the field  $E_x$  increases upto a maximum and then falls down to zero

regularly. With the increase in distortion level, the maximum of  $E_x$  is seen to increase systematically. This observation is clearly exhibited in Fig.(3.10). Also the spread of  $E_x$  field distribution is found to decrease on account of increase in distortion. This is suggestive of more and more confinement of the power near the waveguide axis. For zero relative distortion we have the case of a true parabolic refractive index profile which has the minimum  $E_x$  peak value.

ii) For  $N = 1, 2$  and  $3$  modes with a given distortion in the refractive index profile, the field distributions are oscillatory in character with different number of minima and maxima. Further the minimum of  $E_x$  is found to increase on negative side while maximum of  $E_x$  increases as distortion is gradually increased. Also the field patterns shrink along  $x$ -axis. This indicates a more concentration of the mode power close to the waveguide axis.

From Figs.(3.12)-(3.13) we find that the maxima of  $E_x$  regularly decrease for higher order modes at a given distortion level. Also the effect of increase in distortion is to cause the reduction in the field pattern normally to the guide axis.

b)  $\bar{b} - v$  Curves :

In this case we have employed Eq.(3.32) alongwith definitions of  $2\bar{\Delta}$  and  $\bar{v}$ . The  $\bar{b} - v$  curves have been calculated for different relative distortions. The results are given in Tables (3.7-3.8) and also in Figs.(3.14-3.15).

The following points are found to be noteworthy.

i) For a given TM mode the cut-off frequency value decreases as the relative distortion is increased.

ii) With the increase in mode order the cut-off frequency increases irrespective of the distortion level in the refractive index profile.

iii) With the increase in distortion for a TM mode the saturated part of  $\bar{b} - v$  curves shifts towards higher  $\bar{b}$  values.

### 3.3.3 Group Delay and Radiation Confinement Factor for TE/TM Modes :

a) We have calculated group delays per unit length for TE and TM modes respectively using Eqs.(3.22 and 3.36). The results are presented in Table (3.9) for first four orders.

We list the following observations.

i) For a true parabolic index profile ( $a_1 = 0$ ) it is seen that the group delay per unit length values are the same for both TE and TM modes irrespective of their order. This confirms the TE/TM degeneracy as concluded in Sec.(3.2.2).

ii) With the increase in distortion the group delay value for TE/TM modes increases in the decimal part although its order of magnitude remains the same. Comparatively the increase is significantly more in the case of TE modes. This is true for any order of mode.

iii) For a given distortion irrespective of mode order it is seen that the decimal part of group delay value for TE mode is greater than that for TM mode.

b) The radiation confinement factors ( $\Gamma$ ) for TE/TM modes for  $N = 0$  and  $1$  are calculated employing Eqs.(3.39)-(3.40). The results are given in Table (3.10) and Figs.(3.8)-(3.9).

In Table (3.10) the behaviour of radiation confinement factors with normalise frequency is illustrated for even relative distortion ( $a_1$ ) levels. For either mode, the confinement factor increases rapidly and reaches a saturated value close to unity. This is irrespective of mode order or  $a_1$  values.

From Figs.(3.8) and (3.9) we note that the separation between the  $\Gamma$  vs  $v$  curves for the two modes is markedly more for zero or low distortion levels. With the increase in distortion this difference decreases considerably. For  $a_1 = 0.9$  the two curves almost coincide for initial  $v$  values. It is therefore noted that the confinement factor increases with the increase in distortion for either mode.

#### 3.4 Summary and Conclusions :

At the outset we have established the expression for the parabolic refractive index profile with flat continuation in a form similar to that for a true parabolic refractive index profile. This expression is first used to solve the scalar wave equation for the field distributions

of TE modes. While doing so an effective beam-waist  $w_1$  has been defined in terms of the relative distortion ( $a_1$ ) present in the refractive index profile and the usual beam-waist  $w_0$  found in the literature. The solution for the  $TE_N$  modes are expressed in terms of the Hermite polynomials. The eigenvalue equation is also obtained and is rewritten in terms of a newly defined effective normalised propagation constant. From the eigenvalue equation the expressions for the longitudinal propagation constant  $\beta$  and group delay have been obtained.

The expression for the refractive index for nearly parabolic profile is also used in the scalar equation for electric fields of  $TM_N$  modes. It is solved in a way similar to that adopted for TE case. However, in this case another effective beam-waist  $w_2$  has been defined in terms of  $w_0$  and the relative distortion. The solutions of the wave equation are once again found to be Hermite polynomials. The eigenvalue equation obtained in solving the wave equation has been expressed in an appropriate form so as to plot  $\bar{b} - v$  curves. This is followed by a derivation of the expression for the group delay of  $TM_N$  modes. Finally the expressions for radiation confinement factor are established for zero and first order TE/TM modes.

The expressions for field distribution, normalisation propagation constants, group delay and radiation confinement factors of both the types of modes have been utilised for numerical calculations<sup>6,10</sup>. For this

purpose the software package Lotus-1-2-3 has been utilised with Zenith PC/AT which is available in the Department of Physics, Shivaji University, Kolhapur. All the results have been presented in a number of tables and graphs.

Conclusions :

From the calculated results we list the following findings of the present work.

1) For  $N = 0$  TE/TM mode, the field  $H_x / E_x$  exhibits a Gaussian shape irrespective of the distortion in the refractive index profile. With the increase in distortion level the peak value increases to higher field side. However the shift in  $TE_0$  case is more pronounced as compared to that for  $TM_0$  mode. Also the increase in distortion causes a significant shrink of the  $TE_0$  field patterns towards the waveguide axis. This effect is small for  $TM_0$  modes. A simultaneous increase in the peak value and reduction in the field spreading favours for more confinement of the mode power near the waveguide axis.

2) The field patterns for higher order TE/TM modes exhibit oscillatory character with different number of minima and maxima independent of the distortion level present in the refractive index profile. With the increase in distortion a minimum of the field  $H_x / E_x$  is seen to shift towards negative values, while a maximum increases regularly. This effect is found to be more significant in the case of field patterns for TE modes. Also the spatial extent of field patterns is seen to decrease toward

waveguide axis. This once again suggests for the power confinement close to the waveguide axis.

3) From the study of  $\bar{b} - v$  curves for either type of modes we note that the cut-off frequency decreases to zero as distortion in the refractive index profile increases. For a given distortion the cut-off frequency increases with the increase in mode order. Also for a given mode the asymptotic part of the curve shifts toward  $\bar{b} = 1$  level.

4) In the absence of distortion  $a_1 = 0$  the calculated values of group delay per unit length are found to be the same for both TE and TM modes independent of their order thereby suggesting the TE/TM degeneracy. As the distortion increases the group delay values increase in their decimal parts without any change in the order of magnitude. Comparatively this change is found to be more significant for TE modes. Finally it is noted that the decimal part of a group delay value for a TE mode is greater than that for a TM mode at a given distortion level.

5) The radiation confinement factors for  $N = 0$  and 1 TE/TM modes are found to increase rapidly in the beginning and to reach a saturated unit value at the end. This is more significant for lower distortion levels. At higher relative distortion the initial parts of  $\Gamma$  versus  $v$  curves for  $N = 0$  and 1 modes are more closer. In general the confinement factor is seen to increase with the increase in distortion for either modes.

**References :**

1. Adams M. J. 'An Introduction to Optical Waveguides', (Wiely, New York, 1981), Chap. 3.
2. Sodha M. S. and Ghatak A. K., 'Inhomogeneous Optical Waveguides', (Plenum Press, New York, 1977).
3. Love J. and Ghatak A., IEEE J. Quantum Electron, QE-15, 14, (1979).
4. Keck D. B., Appl. Opt. (USA), 13, 1882, (1974).
5. Ikeda M. and Yoshikyo H., Appl. Opt., (USA), 15, 1307, (1976).
6. Agarwal D. C., Indian J. Phys., 59B, 184, (1985).
7. Marcuse D., 'Light Transmission Optics', (Van Nostrand Reinhold, New York, 1972).
8. Ghatak A. K. and Thyagarajan K., 'Optical Electronics', (Cambridge University Press, 1991).
9. Ghatak A. K. and Kraus L. A., IEEE J. Quantum Electron, QE-10, 465, (1974).
10. Marcuse D., IEEE J. Quantum Electron, QE-9, 958, (1973a)
11. Abramowitz M. and Stegun I. A. 'Handbook of Mathematical Functions', New York, (1964).

**Table 3.1** : Calculated Field Distributions for  
TE<sub>0</sub> and TE<sub>1</sub> modes.

N = 0					
a/ρ = a <sub>1</sub>	x	0	0.2	0.6	0.8
		H <sub>x</sub> →			
-0.00003	0.034859	0.029102	0.003884	0.000098	
-0.000025	0.545292	0.481807	0.120857	0.009605	
-0.00002	5.173591	4.788354	2.012450	0.408446	
-0.000015	29.77196	28.56759	17.93677	7.547930	
-0.00001	103.9143	102.3142	85.57155	60.61890	
-0.000005	219.9866	219.9751	218.5146	211.5807	
0	282.4685	283.9135	298.6740	320.9461	
0.000005	219.9866	219.9751	218.5146	211.5807	
0.00001	103.9143	102.3142	85.57155	60.61890	
0.000015	29.77196	28.56759	17.93677	7.547930	
0.00002	5.173591	4.788354	2.012450	0.408446	
0.000025	0.545292	0.481807	0.120857	0.009605	
0.00003	0.034859	0.029102	0.003884	0.000098	

N = 1					
a/ρ = a <sub>1</sub>	x	0	0.2	0.6	0.8
		H <sub>x</sub> →			
-0.00003	-0.20915	-0.17640	-0.02606	-0.00076	
-0.00002	-20.6943	-19.3498	-8.99995	-2.10921	
-0.000015	-89.3158	-86.5819	-60.1617	-29.2330	
-0.00001	-207.828	-206.727	-191.343	-156.517	
-0.000007	-242.266	-243.530	-253.381	-256.336	
-0.000006	-236.485	-238.357	-255.506	-272.873	
-0.000001	-55.9315	-56.7826	-65.9559	-81.4982	
0	0	0	0	0	
0.000001	55.93157	56.78267	65.95593	81.49826	
0.000006	236.4859	238.3579	255.5060	272.8733	
0.000007	242.2667	243.5307	253.3816	256.3367	
0.00001	207.8287	206.7275	191.3438	156.5173	
0.000015	89.31588	86.58191	60.16176	29.23301	
0.00002	20.69436	19.34989	8.999950	2.109211	
0.00003	0.209156	0.176408	0.026060	0.000760	

**Table 3.2 : Calculated Field Distributions for  
TE<sub>2</sub> and TE<sub>3</sub> modes.**

N = 2					
a/ρ = a <sub>1</sub>	=	0	0.2	0.6	0.8
x	H <sub>x</sub> →				
-0.00003	0.862725	0.735537	0.120871	0.004095	
-0.00002	54.87422	51.90528	27.03732	7.412934	
-0.000012	225.2568	225.2693	216.4433	177.0552	
-0.000011	228.7125	230.0452	235.0192	213.4541	
-0.00001	220.4356	223.0087	242.0329	242.8962	
-0.000009	199.0327	202.6052	234.0233	258.8644	
-0.000008	164.2975	168.4879	208.7707	255.1376	
-0.000001	-189.838	-190.605	-198.142	-208.312	
0	-199.735	-200.757	-211.194	-226.943	
0.000001	-189.838	-190.605	-198.142	-208.312	
0.000008	164.2975	168.4879	208.7707	255.1376	
0.000009	199.0327	202.6052	234.0233	258.8644	
0.00001	220.4356	223.0087	242.0329	242.8962	
0.000011	228.7125	230.0452	235.0192	213.4541	
0.000012	225.2568	225.2693	216.4433	177.0552	
0.00002	54.87422	51.90528	27.03732	7.412934	
0.00003	0.862725	0.735537	0.120871	0.004095	

N = 3					
a/ρ = a <sub>1</sub>	=	0	0.2	0.6	0.8
x	H <sub>x</sub> →				
-0.00003	-2.81779	-2.43007	-0.44685	-0.01769	
-0.000025	-24.4876	-22.3708	-7.79183	-0.97878	
-0.00002	-109.829	-105.300	-62.4616	-20.3789	
-0.000015	-218.778	-218.641	-202.627	-143.211	
-0.000014	-220.130	-221.842	-223.986	-181.814	
-0.000013	-208.016	-211.553	-233.614	-217.431	
-0.000012	-180.980	-186.072	-227.147	-243.068	
-0.000011	-139.199	-145.341	-201.571	-250.956	
-0.00001	-84.8457	-91.3574	-156.231	-234.292	
-0.000004	185.5279	186.7193	196.4403	200.3852	
-0.000003	166.9410	168.7261	186.3846	209.6521	
0	0	0	0	0	
0.000003	-166.941	-168.726	-186.384	-209.652	
0.000004	-185.527	-186.719	-196.440	-200.385	
0.00001	84.84571	91.35741	156.2315	234.2924	
0.000011	139.1997	145.3419	201.5714	250.9566	
0.000012	180.9800	186.0723	227.1471	243.0688	
0.000013	208.0165	211.5538	233.6144	217.4312	
0.000014	220.1306	221.8429	223.9867	181.8148	
0.000015	218.7783	218.6414	202.6277	143.2119	
0.00002	109.8297	105.3005	62.46164	20.37893	
0.000025	24.48762	22.37084	7.791834	0.978783	
0.00003	2.817794	2.430074	0.446852	0.017696	

**Table 3.3** : Calculation of  $\beta - v$  curves for  $TE_0$  and  $TE_1$  modes.

$N$	$=$	$0$			
$a/\rho = a_1$	$=$	$0$	$0.2$	$0.6$	$0.8$
$v$		$\beta \longrightarrow$			
0.4		-1.5	-1.44948	-1	-0.5
1		0	0.020204	0.2	0.4
2		0.5	0.510102	0.6	0.7
3	0.666666	0.673401	0.733333		0.8
4		0.75	0.755051	0.8	0.85
5		0.8	0.804040	0.84	0.88
6	0.833333	0.836700	0.866666		0.9
7	0.857142	0.860029	0.885714	0.914285	
8		0.875	0.877525	0.9	0.925
9	0.888888	0.891133	0.911111	0.933333	
10		0.9	0.902020	0.92	0.94

$N$	$=$	$1$			
$a/\rho = a_1$	$=$	$0$	$0.2$	$0.6$	$0.8$
$v$		$\beta \longrightarrow$			
0.4		-6.5	-6.34846	-5	-3.5
1		-2	-1.93938	-1.4	-0.8
2		-0.5	-0.46969	-0.2	0.1
3		0	0.020204	0.2	0.4
4		0.25	0.265153	0.4	0.55
5		0.4	0.412122	0.52	0.64
6		0.5	0.510102	0.6	0.7
7	0.571428	0.580087	0.657142	0.742857	
8		0.625	0.632576	0.7	0.775
9	0.666666	0.673401	0.733333		0.8
10		0.7	0.706061	0.76	0.82

**Table 3.4 :** Calculation of  $\bar{B} - v$  curves for  $TE_2$  and  $TE_3$  modes.

$N = 2$					
$a/\rho = a_1 =$	$v$	0	0.2	0.6	0.8
		$\bar{B} \longrightarrow$			
0.4		-11.5	-11.2474	-9	-6.5
1		-4	-3.89897	-3	-2
2		-1.5	-1.44948	-1	-0.5
3		-0.66666	-0.63299	-0.33333	2.1E-16
4		-0.25	-0.22474	7.2E-17	0.25
5		0	0.020204	0.2	0.4
6		0.166666	0.183503	0.333333	0.5
7		0.285714	0.300145	0.428571	0.571428
8		0.375	0.387627	0.5	0.625
9		0.444444	0.455668	0.555555	0.666666
10		0.5	0.510102	0.6	0.7

$N = 3$					
$a/\rho = a_1 =$	$v$	0	0.2	0.6	0.8
		$\bar{B} \longrightarrow$			
0.4		-16.5	-16.1464	-13	-9.5
1		-6	-5.85857	-4.6	-3.2
2		-2.5	-2.42928	-1.8	-1.1
3		-1.33333	-1.28619	-0.86666	-0.4
4		-0.75	-0.71464	-0.4	-0.05
5		-0.4	-0.37171	-0.12	0.16
6		-0.16666	-0.14309	0.066666	0.3
7		0	0.020204	0.2	0.4
8		0.125	0.142678	0.3	0.475
9		0.222222	0.237936	0.377777	0.533333
10		0.3	0.314142	0.44	0.58

**Table 3.5 : Calculated Field Distributions for  $TM_0$  and  $TM_1$  modes.**

$N = 0$					
$a/\rho = a_1 =$	0	0.2	0.6	0.8	
x	$E_x \rightarrow$				
-0.000013	0.080132	0.068555	0.021575	0.008714	
-0.000011	0.805775	0.721607	0.318391	0.167478	
-0.000001	2.211902	2.020867	1.033703	0.610352	
-0.000008	12.49019	11.80945	7.782905	5.602201	
-0.000006	48.00706	46.61715	37.41580	31.41853	
-0.000004	125.5953	124.3041	114.8513	107.6620	
-0.000002	223.6530	223.8976	225.1047	225.4180	
-0.000001	258.3598	259.3824	266.3463	271.1565	
0	271.0868	272.4191	281.7090	288.3792	
0.000001	258.3598	259.3824	266.3463	271.1565	
0.000002	223.6530	223.8976	225.1047	225.4180	
0.000004	125.5953	124.3041	114.8513	107.6620	
0.000006	48.00706	46.61715	37.41580	31.41853	
0.000008	12.49019	11.80945	7.782905	5.602201	
0.000001	2.211902	2.020867	1.033703	0.610352	
0.000011	0.805775	0.721607	0.318391	0.167478	
0.000013	0.080132	0.068555	0.021575	0.008714	

$N = 1$					
$a/\rho = a_1 =$	0	0.2	0.6	0.8	
x	$E_x \rightarrow$				
-0.000013	-0.45686	-0.39471	-0.13284	-0.05622	
-0.000001	-9.70073	-8.95024	-4.89575	-3.02921	
-0.000007	-78.8782	-76.3976	-59.8375	-49.0189	
-0.0000035	-230.883	-231.587	-234.939	-235.596	
-0.000003	-231.375	-232.799	-241.634	-246.683	
-0.0000025	-220.072	-222.007	-234.937	-243.503	
-0.000002	-196.174	-198.324	-213.224	-223.752	
-0.0000015	-160.048	-162.071	-176.408	-186.909	
-0.000001	-113.308	-114.878	-126.145	-134.576	
-0.0000005	-58.7349	-59.5909	-65.7817	-70.4689	
0	2.5E-14	2.6E-14	2.8E-14	3.0E-14	
0.0000005	58.73490	59.59096	65.78179	70.46892	
0.000001	113.3088	114.8782	126.1450	134.5766	
0.0000015	160.0481	162.0718	176.4082	186.9094	
0.000002	196.1749	198.3246	213.2249	223.7526	
0.0000025	220.0724	222.0078	234.9370	243.5031	
0.000003	231.3756	232.7999	241.6345	246.6836	
0.0000035	230.8836	231.5871	234.9390	235.5969	
0.000007	78.87827	76.39761	59.83756	49.01893	
0.000001	9.700737	8.950244	4.895752	3.029217	
0.000013	0.456869	0.394716	0.132841	0.056227	

**Table 3.6 : Calculated Field Distributions for  
TM<sub>2</sub> and TM<sub>3</sub> modes.**

N = 2					
a/ρ = a <sub>1</sub>	= 0	0.2	0.6	0.8	
x	E <sub>x</sub> →				
-0.000013	1.785207	1.558505	0.563086	0.250361	
-0.00001	28.51945	26.60063	15.66468	10.19919	
-0.000008	99.88865	96.48023	73.50146	58.48728	
-0.0000065	179.1206	176.8071	157.9692	142.2242	
-0.000006	201.1091	199.8068	187.1864	174.7867	
-0.0000055	215.6610	215.6025	211.3029	204.2145	
-0.000005	219.4176	220.6921	225.9026	225.5973	
-0.0000045	209.5780	212.0900	226.6713	233.6893	
-0.000003	90.91050	94.82502	122.5125	142.5612	
-0.0000005	-180.289	-180.951	-185.410	-188.434	
0	-191.687	-192.629	-199.198	-203.914	
0.0000005	-180.289	-180.951	-185.410	-188.434	
0.000003	90.91050	94.82502	122.5125	142.5612	
0.0000045	209.5780	212.0900	226.6713	233.6893	
0.000005	219.4176	220.6921	225.9026	225.5973	
0.0000055	215.6610	215.6025	211.3029	204.2145	
0.000006	201.1091	199.8068	187.1864	174.7867	
0.0000065	179.1206	176.8071	157.9692	142.2242	
0.000008	99.88865	96.48023	73.50146	58.48728	
0.00001	28.51945	26.60063	15.66468	10.19919	
0.000013	1.785207	1.558505	0.563086	0.250361	

N = 3					
a/ρ = a <sub>1</sub>	= 0	0.2	0.6	0.8	
x	E <sub>x</sub> →				
-0.000013	-5.50333	-4.85839	-1.89314	-0.88669	
-0.00001	-64.2929	-60.7108	-38.8361	-26.7516	
-0.000007	-206.891	-206.206	-195.212	-181.501	
-0.0000065	-212.071	-213.216	-214.526	-208.577	
-0.000006	-202.389	-205.401	-220.293	-224.112	
-0.000005	-131.915	-137.603	-174.795	-197.889	
-0.0000025	161.5267	160.7895	153.2749	145.1880	
-0.000002	178.6465	179.3705	183.0429	184.0380	
-0.0000015	167.7410	169.2949	179.7077	186.6264	
-0.0000005	70.78227	71.79074	79.05996	84.53488	
0	-3.1E-14	-3.1E-14	-3.5E-14	-3.7E-14	
0.0000005	-70.7822	-71.7907	-79.0599	-84.5348	
0.0000015	-167.741	-169.294	-179.707	-186.626	
0.000002	-178.646	-179.370	-183.042	-184.038	
0.0000025	-161.526	-160.789	-153.274	-145.188	
0.000005	131.9153	137.6033	174.7952	197.8899	
0.000006	202.3899	205.4017	220.2931	224.1121	
0.0000065	212.0714	213.2162	214.5266	208.5774	
0.000007	206.8918	206.2066	195.2123	181.5012	
0.00001	64.29296	60.71080	38.83616	26.75164	
0.000013	5.503339	4.858399	1.893148	0.886697	

**Table 3.7 :** Calculation of  $\bar{B} - v$  curves for  $TM_0$  and  $TM_1$  modes.

$N$	$= 0$			
$a/\rho = a_1$	$0$	$0.2$	$0.6$	$0.8$
$v$	$\bar{B} \longrightarrow$			
0.4	-1.53630	-1.48575	-1.03576	-0.53476
1	-0.00592	0.014287	0.194136	0.394250
2	0.498510	0.508613	0.598522	0.698547
3	0.666003	0.672738	0.732675	0.799352
4	0.749626	0.754677	0.799629	0.849635
5	0.799760	0.803801	0.839762	0.879766
6	0.833167	0.836534	0.866501	0.899837
7	0.857020	0.859907	0.885593	0.914166
8	0.874906	0.877432	0.899907	0.924908
9	0.888814	0.891059	0.911037	0.933261
10	0.899940	0.901960	0.919940	0.939941

$N$	$= 1$			
$a/\rho = a_1$	$0$	$0.2$	$0.6$	$0.8$
$v$	$\bar{B} \longrightarrow$			
0.4	-6.53406	-6.38244	-5.03298	-3.53110
1	-2.00577	-1.94515	-1.40568	-0.80551
2	-0.50147	-0.47116	-0.20145	0.098576
3	-0.00065	0.019546	0.199348	0.399360
4	0.249628	0.264782	0.399632	0.549638
5	0.399761	0.411884	0.519763	0.639768
6	0.499834	0.509936	0.599835	0.699838
7	0.571306	0.579965	0.657022	0.742738
8	0.624906	0.632483	0.699907	0.774908
9	0.666592	0.673327	0.733260	0.799928
10	0.699940	0.706001	0.759940	0.819941

**Table 3.8 :** Calculation of  $\bar{b} - v$  curves for  $TM_2$  and  $TM_3$  modes.

$v$	$\bar{b} \longrightarrow$			
	0	0.2	0.6	0.8
0.4	-11.5318	-11.2791	-9.03019	-6.52744
1	-4.00563	-3.90460	-3.00550	-2.00528
2	-1.50145	-1.45094	-1.00143	-0.50139
3	-0.66731	-0.63364	-0.33397	-0.00063
4	-0.25036	-0.22511	-0.00036	0.249642
5	-0.00023	0.019967	0.199765	0.399769
6	0.166501	0.183338	0.333170	0.499839
7	0.285593	0.300024	0.428451	0.571310
8	0.374907	0.387534	0.499907	0.624909
9	0.444370	0.455595	0.555482	0.666595
10	0.499940	0.510042	0.599940	0.699941

$v$	$\bar{b} \longrightarrow$			
	0	0.2	0.6	0.8
0.4	-16.5295	1.423461	-13.0274	-9.52379
1	-6.00549	2.165433	-4.60532	-3.20504
2	-2.50143	3.797435	-1.80141	-1.10136
3	-1.33398	6.244083	-0.86730	-0.40062
4	-0.75036	10.31812	-0.40036	-0.05035
5	-0.40023	18.45227	-0.12023	0.159771
6	-0.16683	42.74330	0.066504	0.299840
7	-0.00012	-352420.	0.199880	0.399882
8	0.124907	-55.4257	0.299908	0.474909
9	0.222148	-30.6318	0.377705	0.533262
10	0.299940	-22.4045	0.439941	0.579942

**Table 3.9 : Calculated Group Delay/unit length for TE/TM modes.**

$\frac{N}{a/\rho = a_1} =$	0	0.2	0.6	0.8
TE : $\tau_g / L =$	5.1433E-09	5.1500E-09	5.2335E-09	5.4283E-09
TM : $\tau_g / L =$	5.1433E-09	5.1438E-09	5.1490E-09	5.1611E-09
$\frac{N}{a/\rho = a_1} =$	1	0.2	0.6	0.8
TE : $\tau_g / L =$	5.1433E-09	5.1500E-09	5.2335E-09	5.4283E-09
TM : $\tau_g / L =$	5.1433E-09	5.1438E-09	5.1490E-09	5.1611E-09
$\frac{N}{a/\rho = a_1} =$	2	0.2	0.6	0.8
TE : $\tau_g / L =$	5.1433E-09	5.1500E-09	5.2335E-09	5.4283E-09
TM : $\tau_g / L =$	5.1433E-09	5.1438E-09	5.1490E-09	5.1611E-09
$\frac{N}{a/\rho = a_1} =$	3	0.2	0.6	0.8
TE : $\tau_g / L =$	5.1433E-09	5.1500E-09	5.2335E-09	5.4283E-09
TM : $\tau_g / L =$	5.1434E-09	5.1438E-09	5.1490E-09	5.1611E-09

**Table 3.10** : Calculated Confinement factors for TE/TM modes.

N	=	0	1	0	1
$a/\rho = a_1 =$		0		0.2	
v		$\Gamma_0$	$\Gamma_1$	$\Gamma_0$	$\Gamma_1$
1		-0.23235038	-0.64745788	-0.10980494	-0.52061144
2		0.939892869	0.723929003	0.943967763	0.734603598
3		0.984946356	0.887642010	0.986026161	0.893620617
4		0.995255826	0.953921856	0.995673999	0.957222131
5		0.998426582	0.981425848	0.998593787	0.983101251
6		0.999466818	0.992615663	0.999533168	0.993417228
7		0.999816991	0.997094649	0.999843041	0.997462440
8		0.999936620	0.998865979	0.999946755	0.999029621
9		0.999977902	0.999560143	0.999981815	0.999631258
10		0.999992254	0.999830256	0.999993756	0.999860592

N	=	0	1	0	1
$a/\rho = a_1 =$		0.6		0.8	
v		$\Gamma_0$	$\Gamma_1$	$\Gamma_0$	$\Gamma_1$
1		0.594025217	0.232580431	0.883161378	0.608020386
2		0.971647313	0.825197488	0.989857617	0.916364586
3		0.993712578	0.942324026	0.998426582	0.981425848
4		0.998426582	0.981425848	0.999738916	0.996031145
5		0.999592303	0.994146592	0.999955421	0.999172454
6		0.999892404	0.998183266	0.999992254	0.999830256
7		0.999971258	0.999442347	0.999998637	0.999965588
8		0.999992254	0.999830256	0.999999758	0.999993085
9		0.999997898	0.999948669	0.999999956	0.999998619
10		0.999999426	0.999984559	0.999999992	0.999999726

Fig.3.1 : Parabolic Refractive Index Profile with Flat Continuation  
( $a_1 = 0.3$  and  $0.7$ )

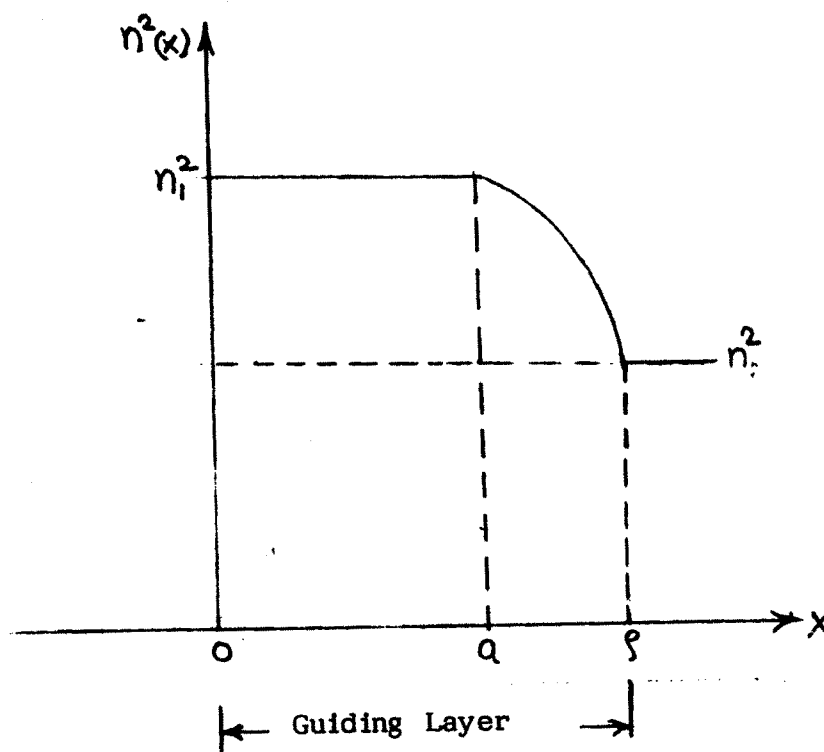
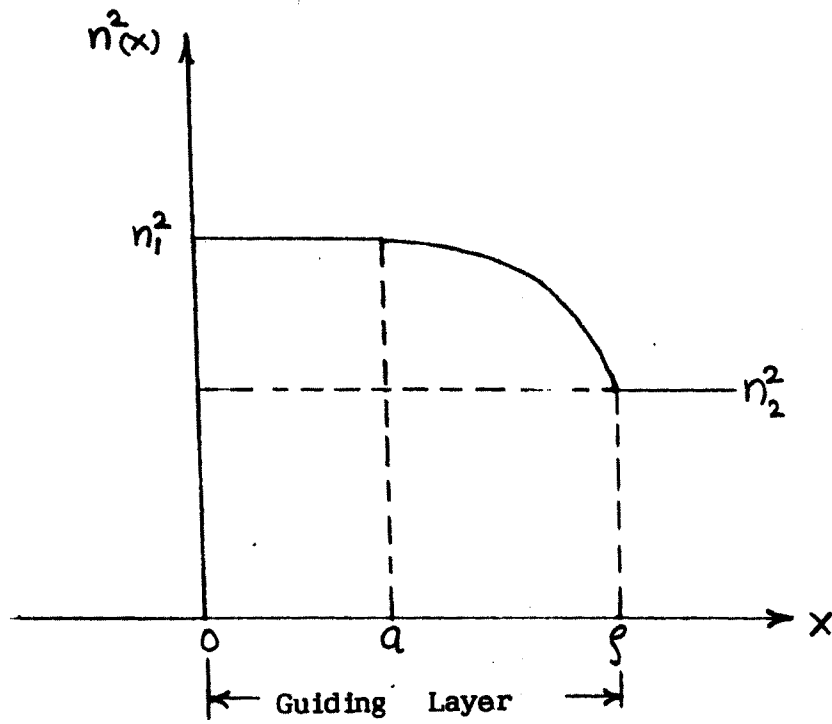


Fig 3.2 : Field distributions for  $TE_0$  and  $TE_1$  modes.

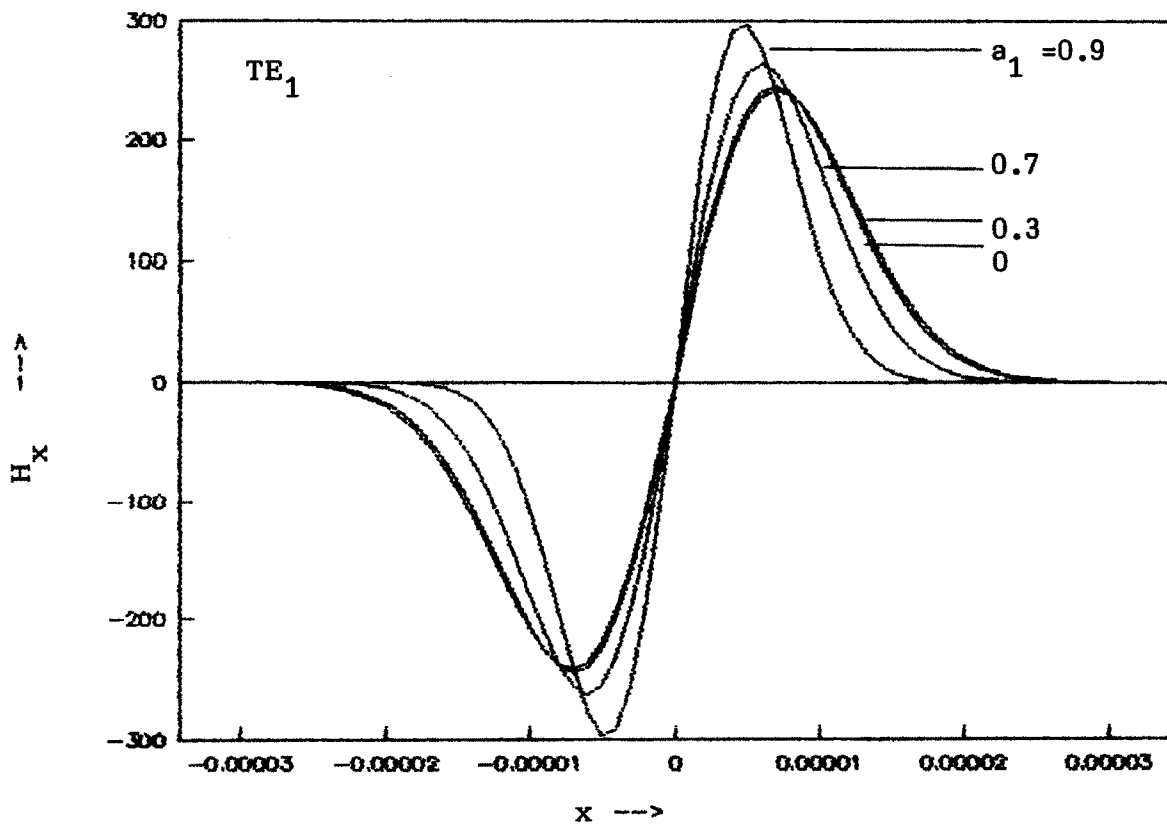
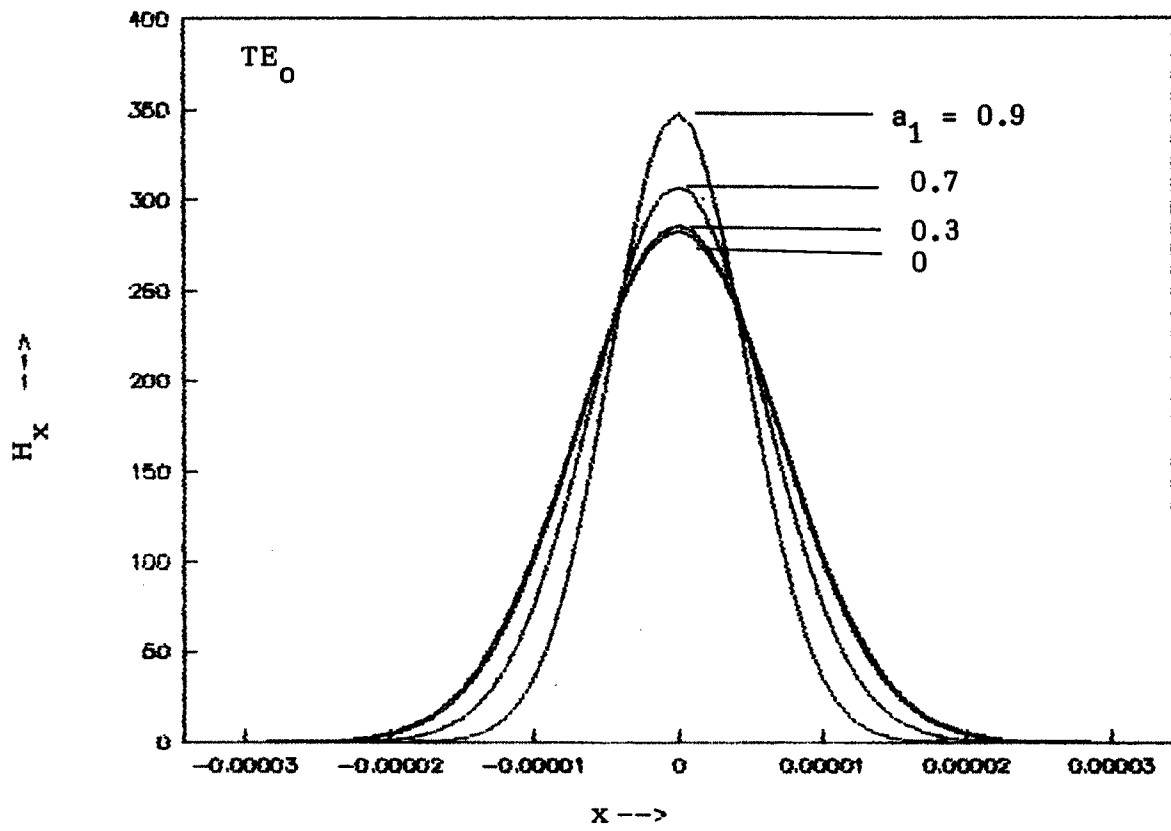
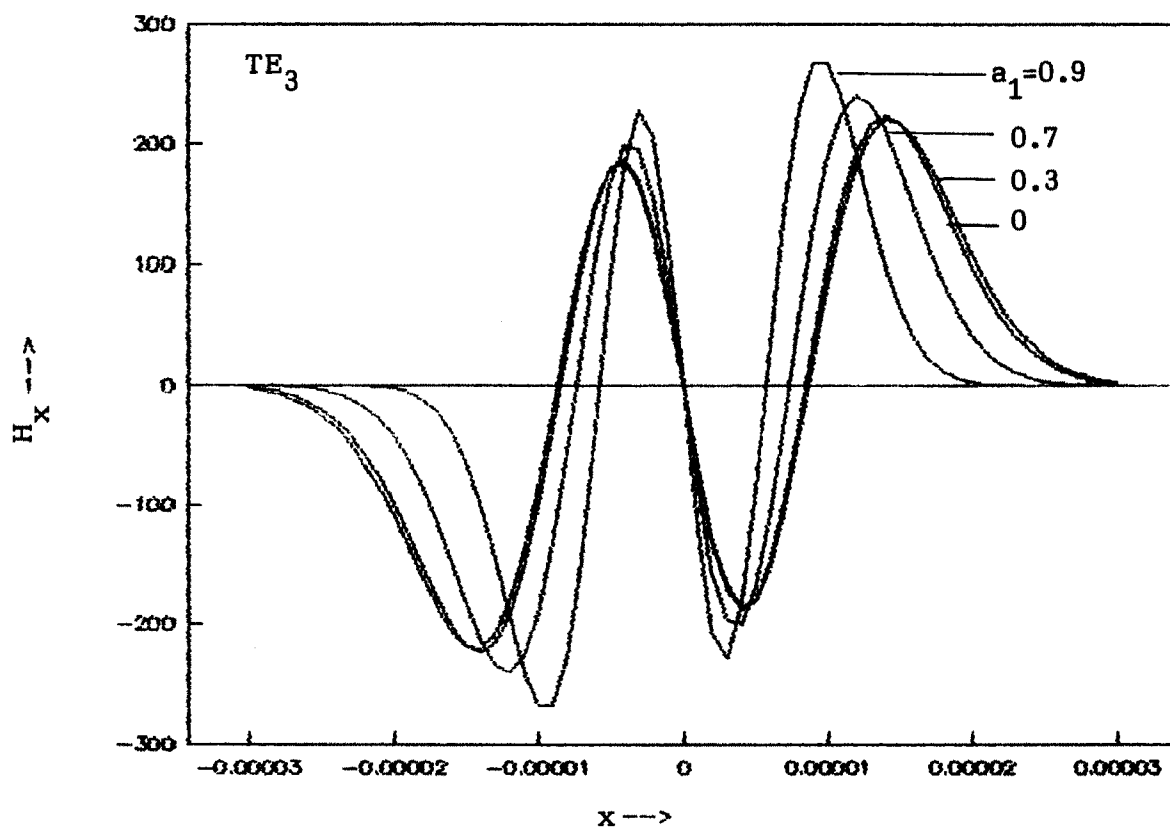
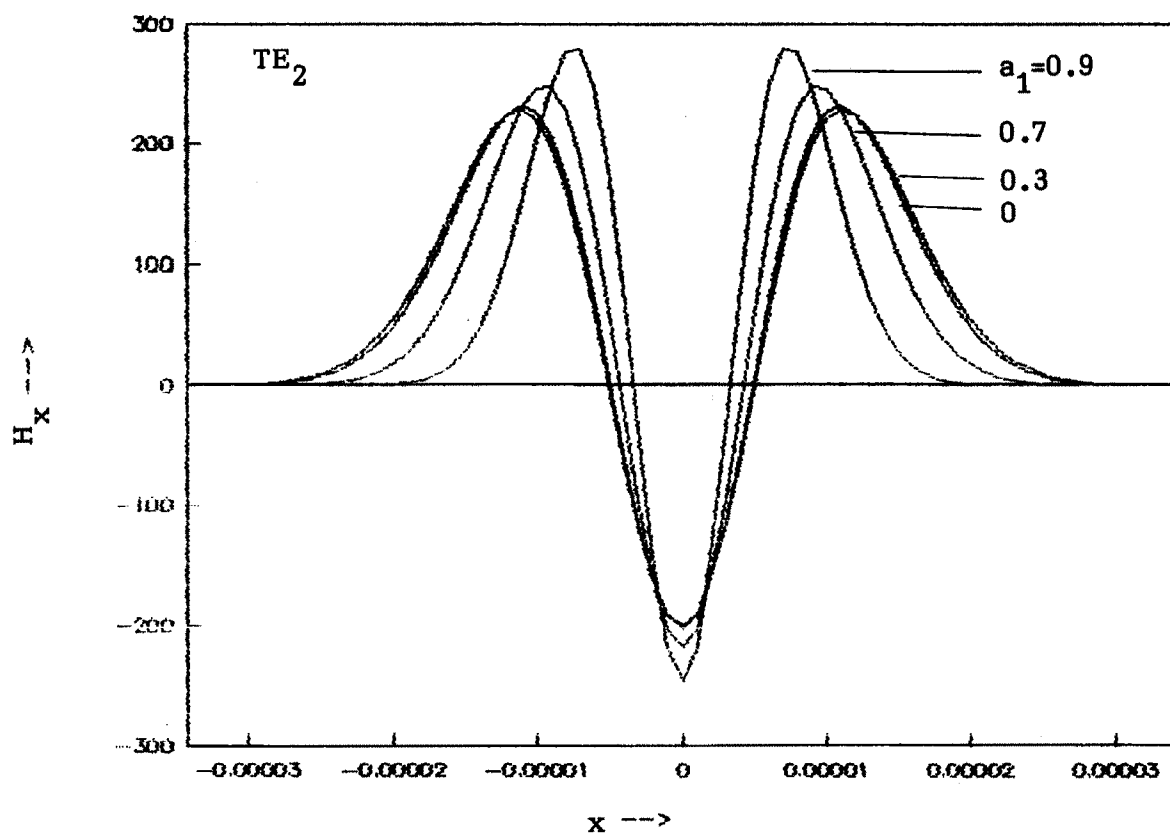
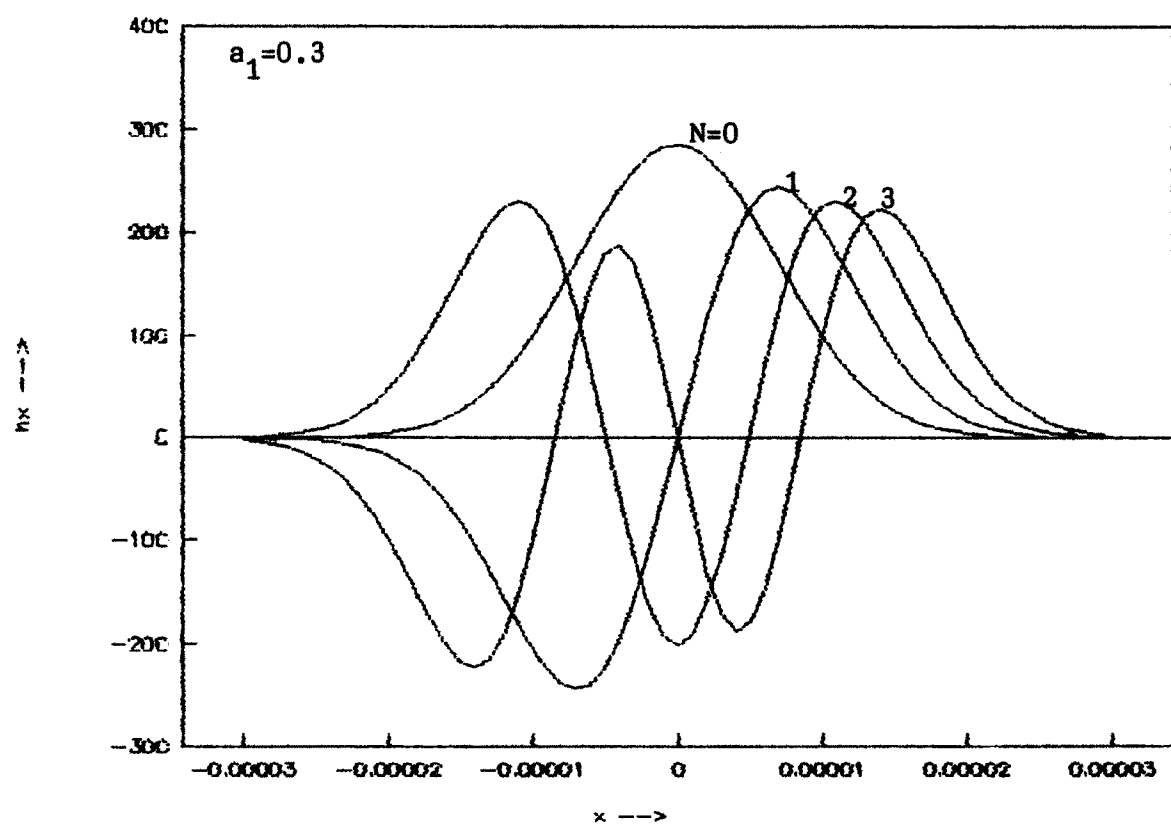
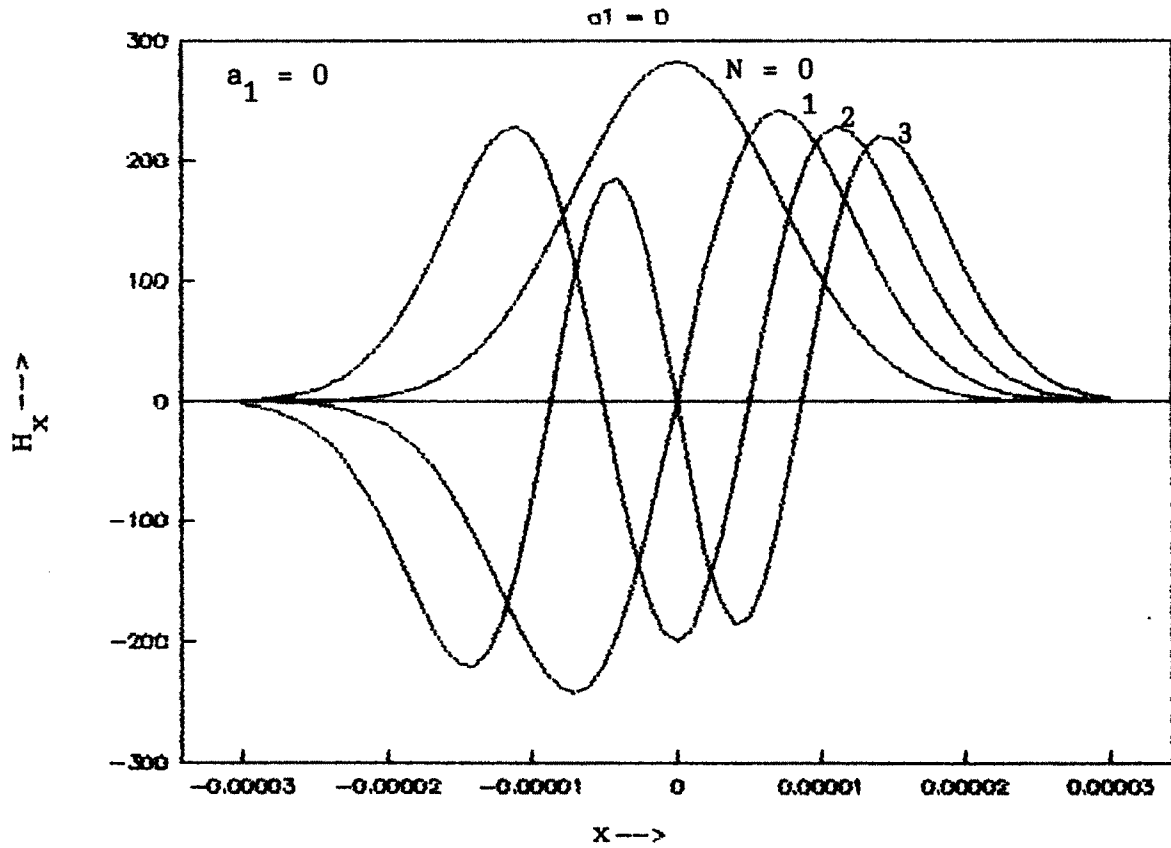


Fig 3.3 : Field distributions for  $TE_2$  and  $TE_3$  modes.



**Fig 3.4 :** Comparative Field distributions of TE modes for  $a/\rho = 0$  and  $0.3$  .



**Fig 3.5** : Comparative Field distributions of TE modes for  $a/\rho = 0.7$  and  $0.9$  .

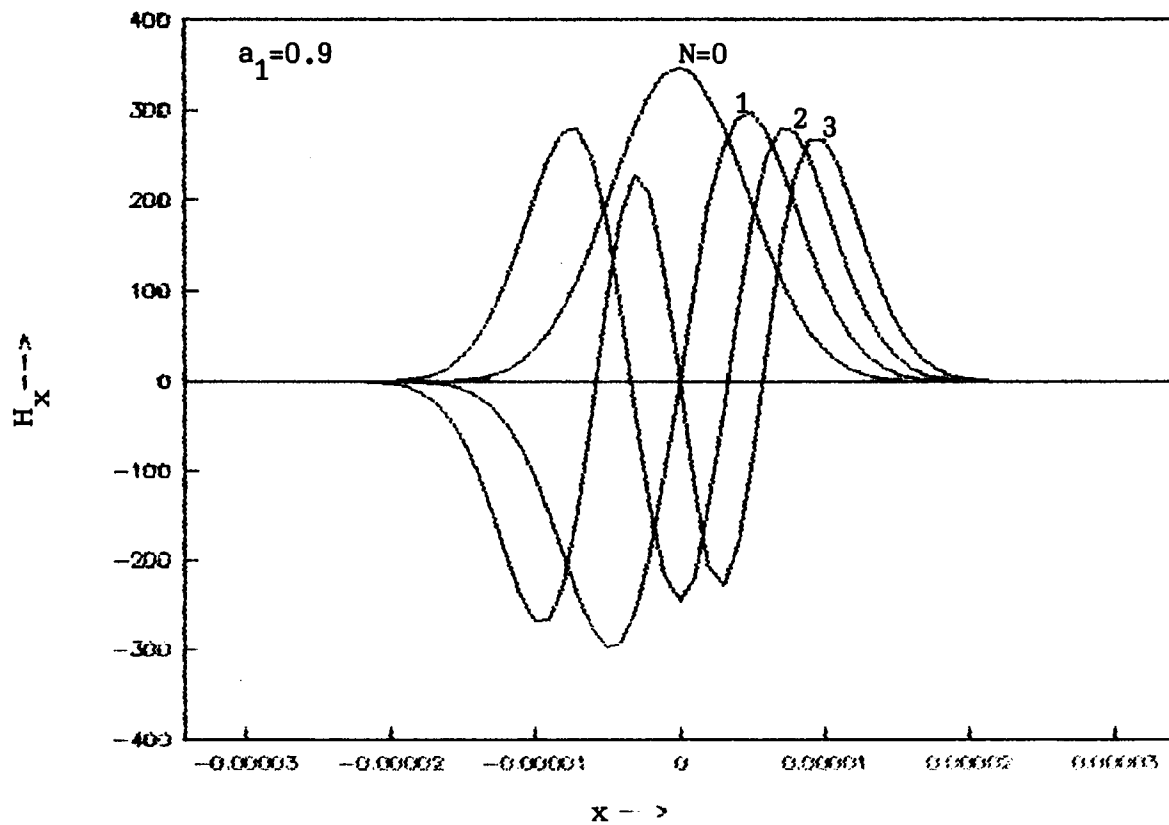
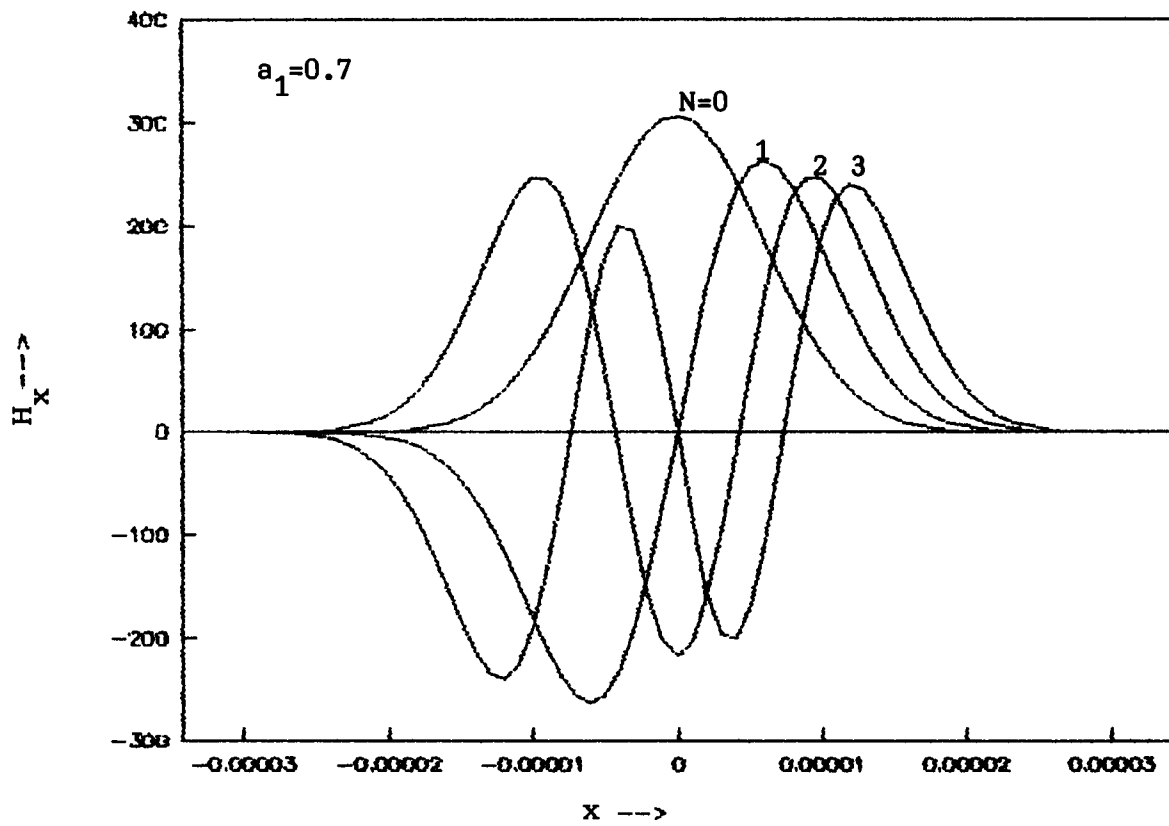


Fig 3.6 :  $\bar{b} - v$  curves for  $TE_0$  and  $TE_1$  modes.

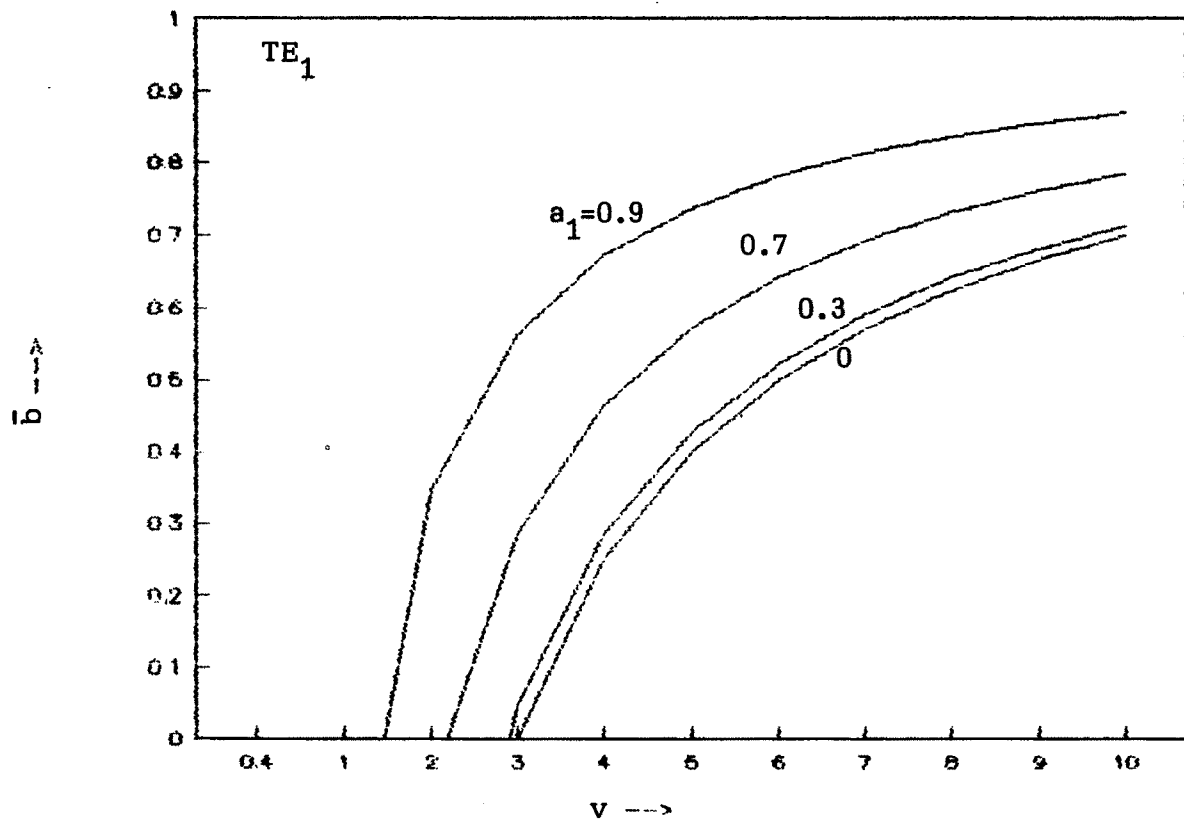
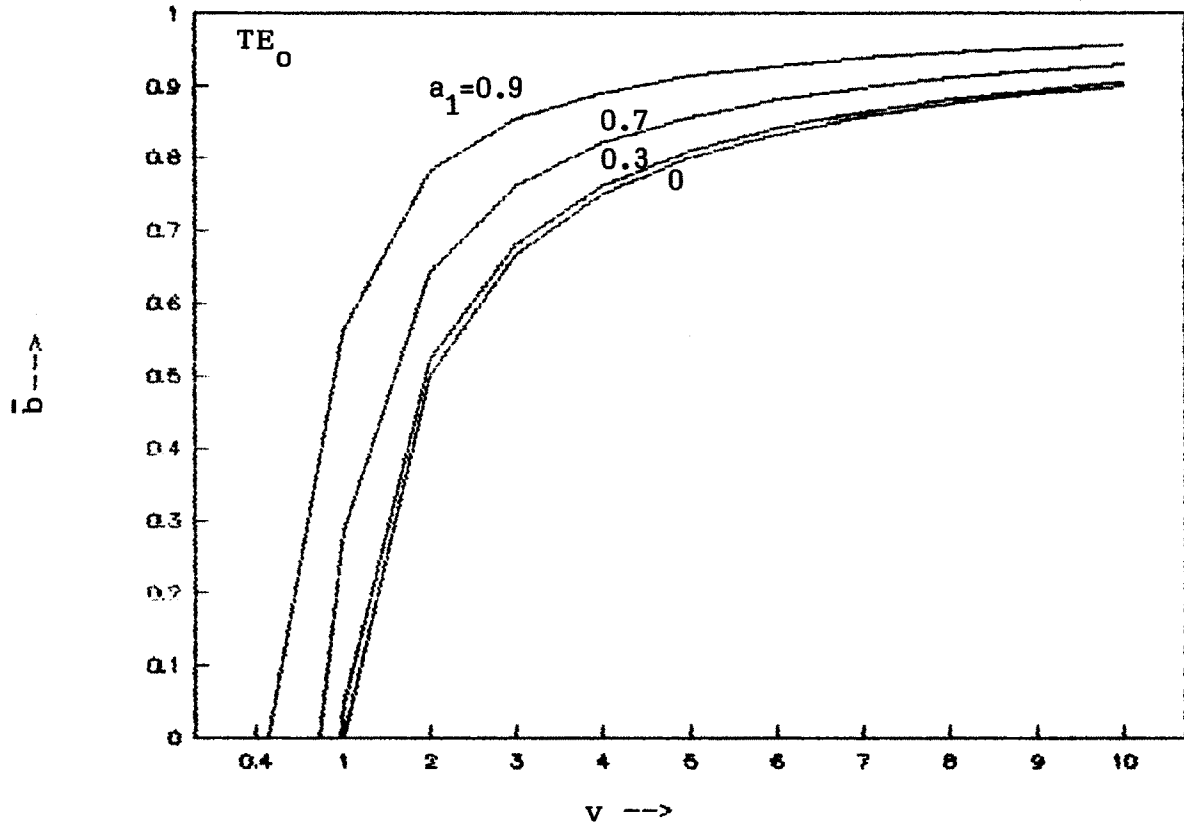


Fig 3.7 :  $\bar{b} - v$  curves for  $TE_2$  and  $TE_3$  modes.

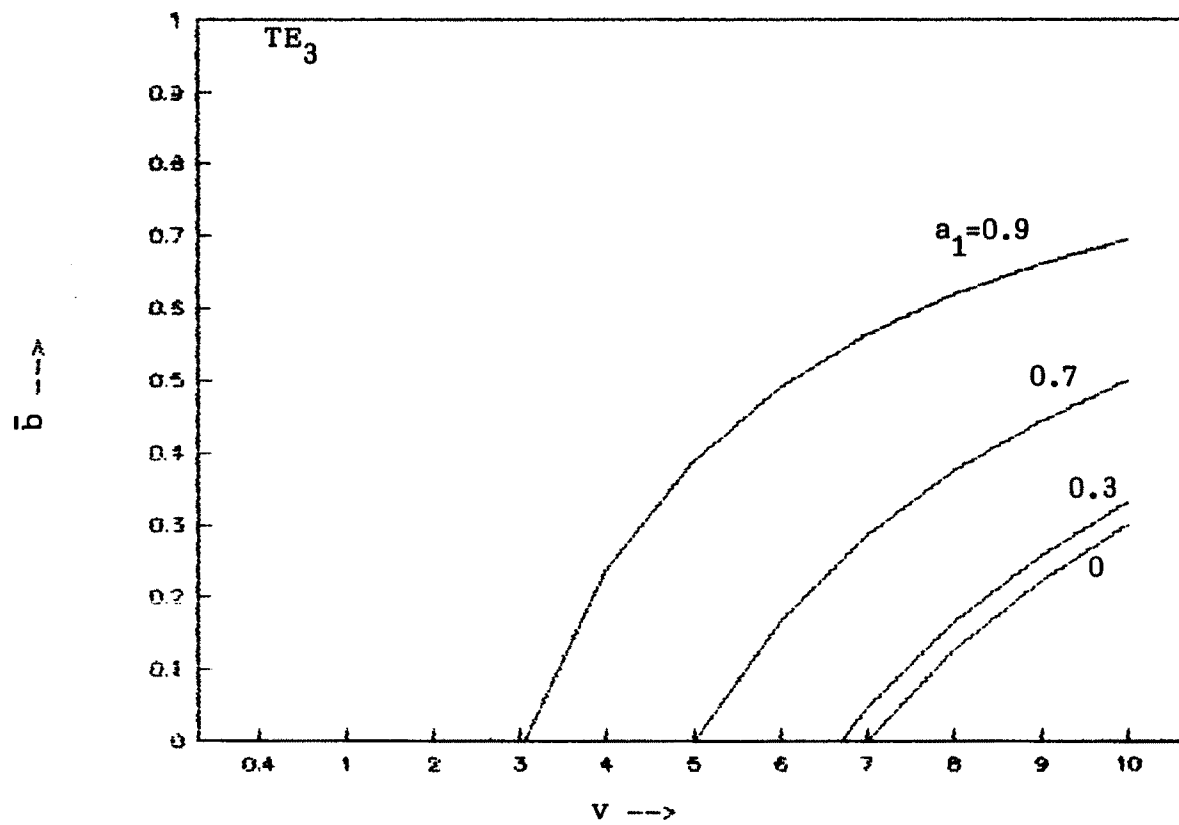
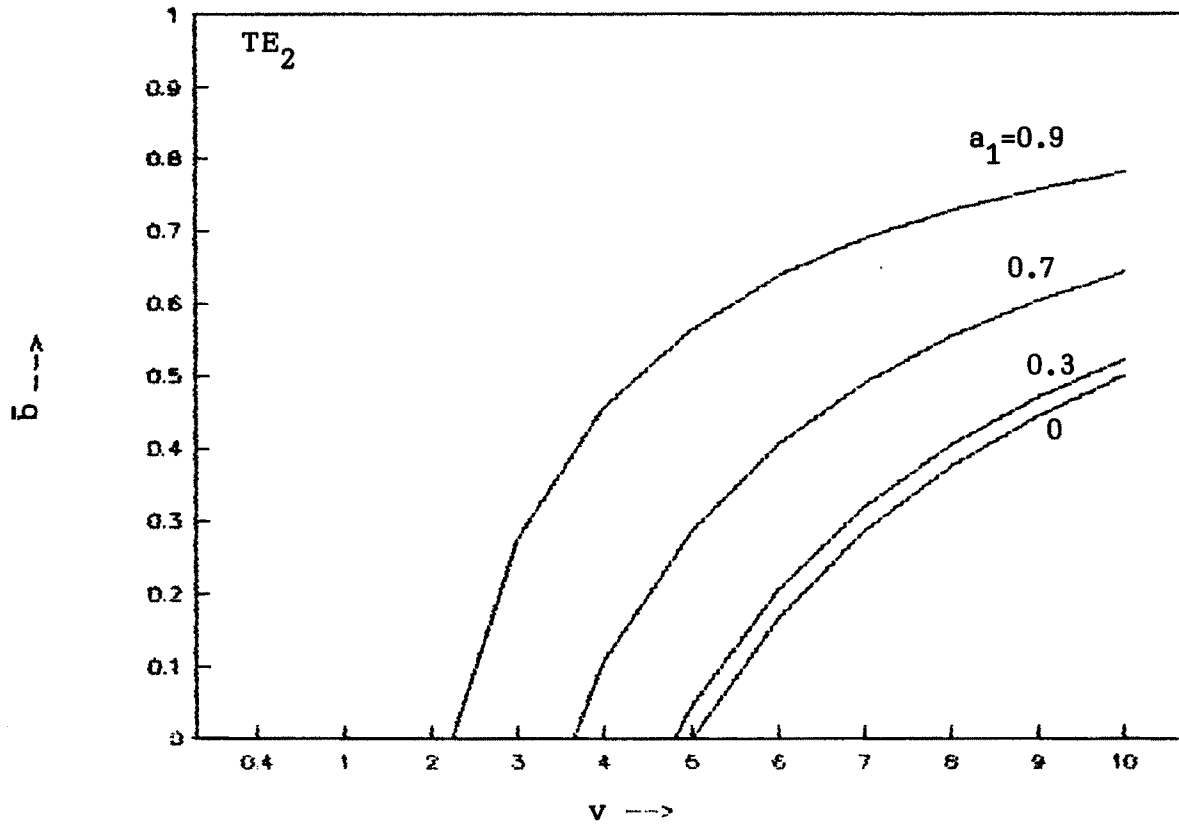
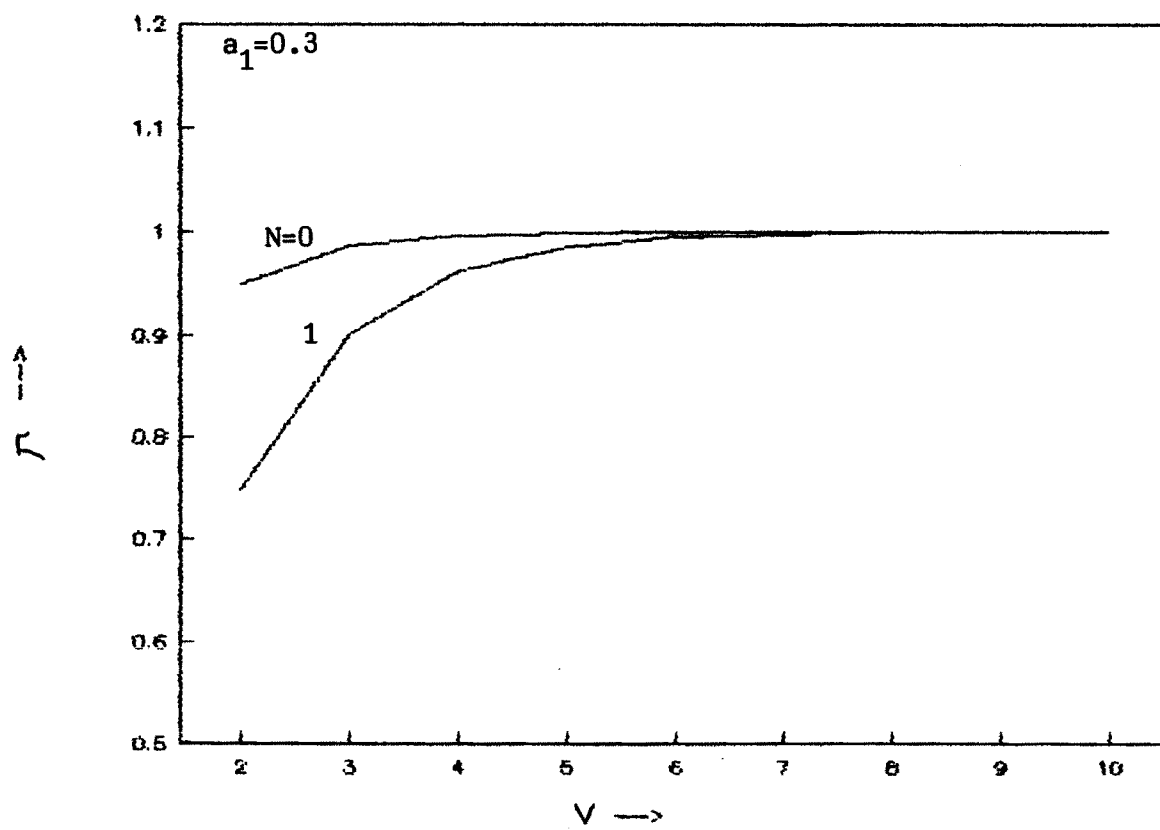
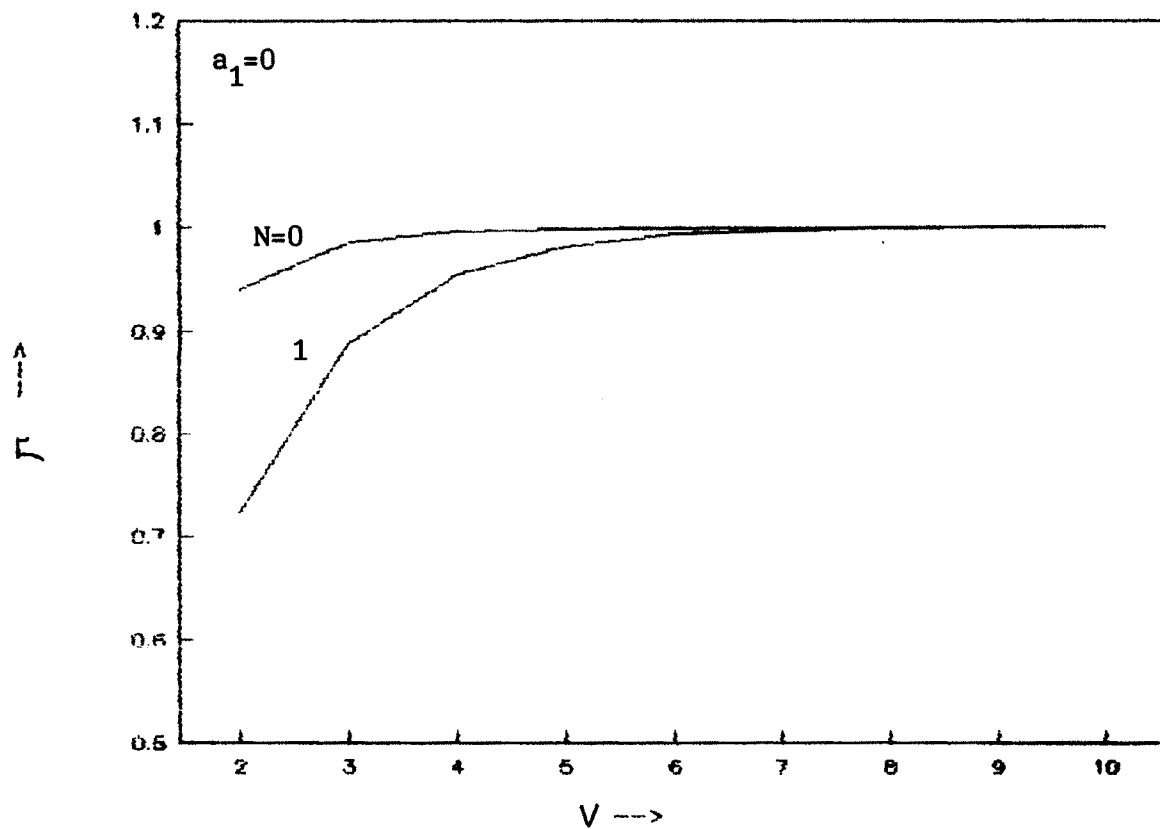


Fig 3.8 : Radiation Confinement Factor Plots for TE/TM modes



**Fig 3.9 : Radiation Confinement Factor Plots for TE/TM modes**

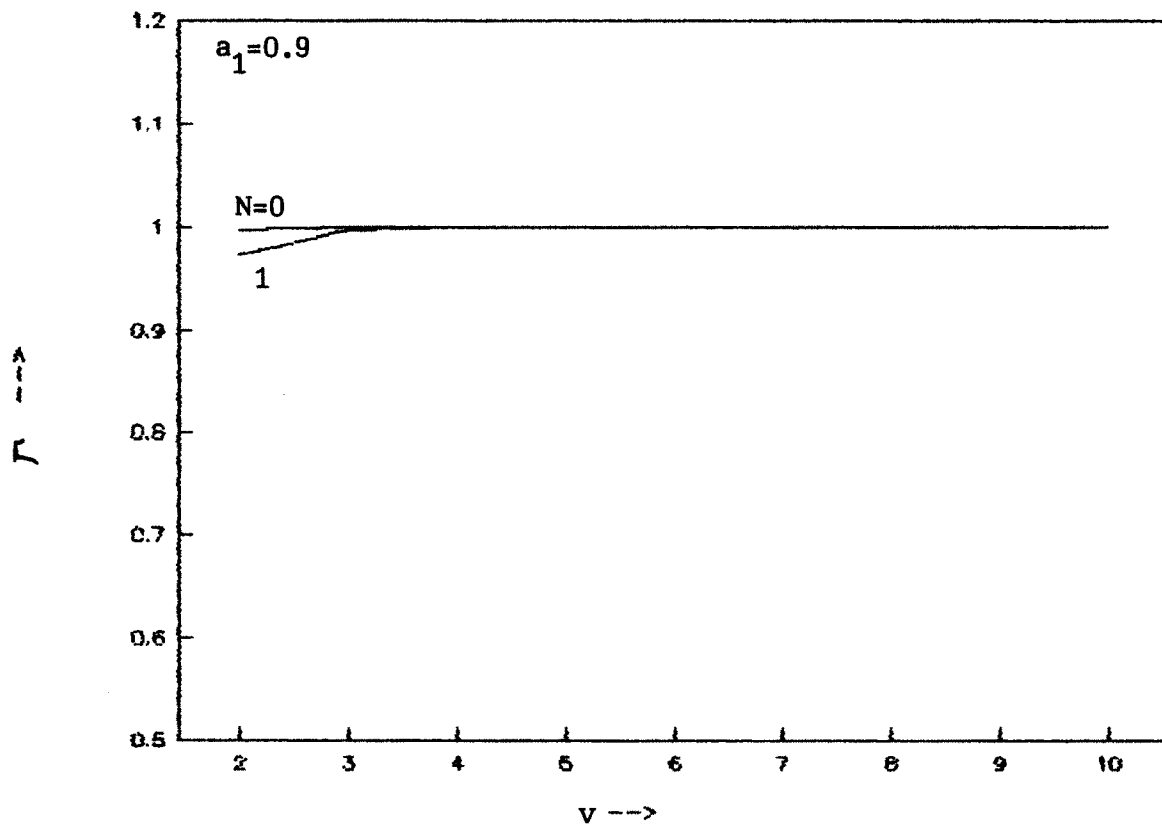
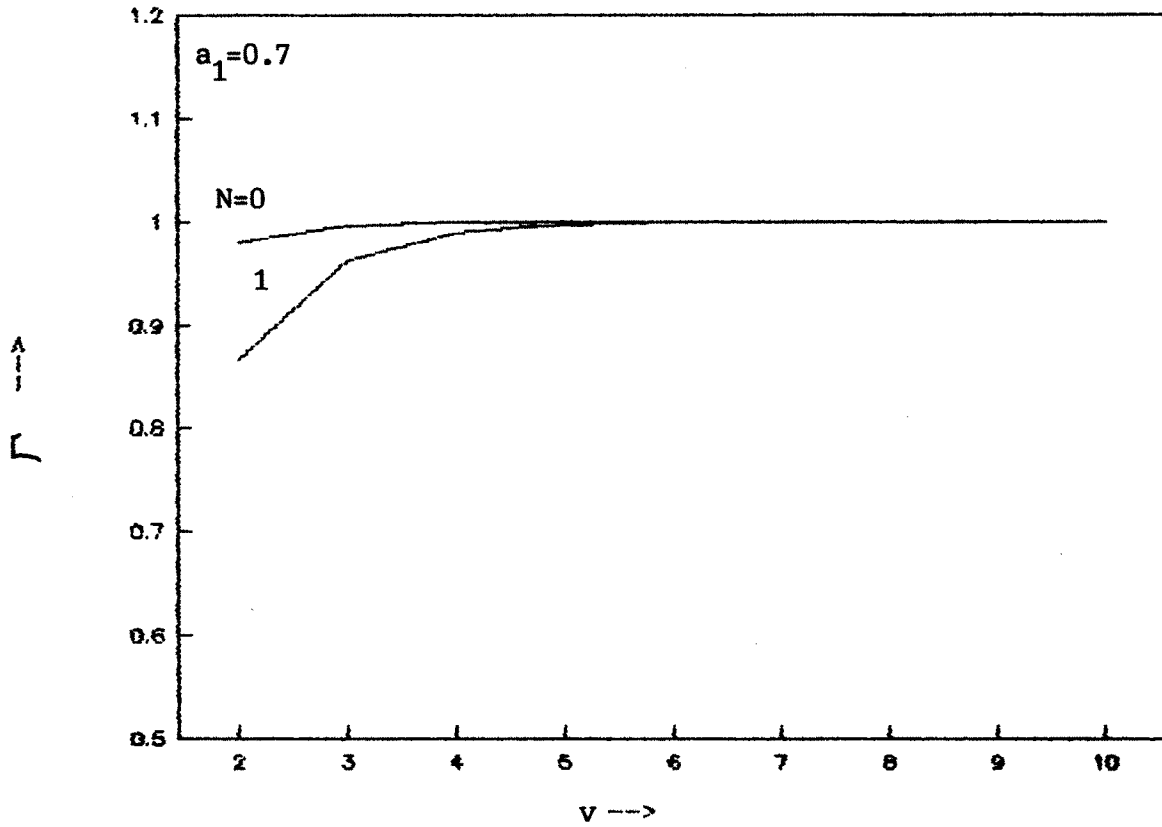


Fig 3.10 : Field distributions for  $TM_0$  and  $TM_1$  modes.

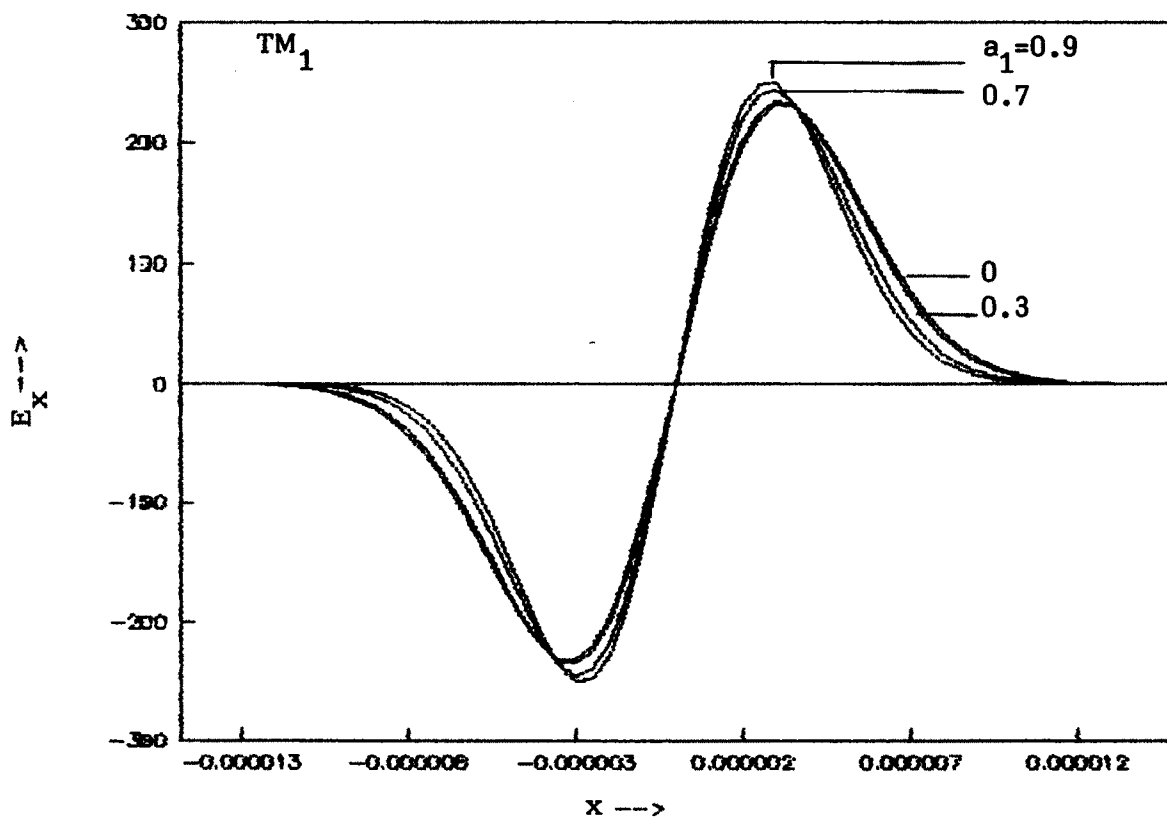
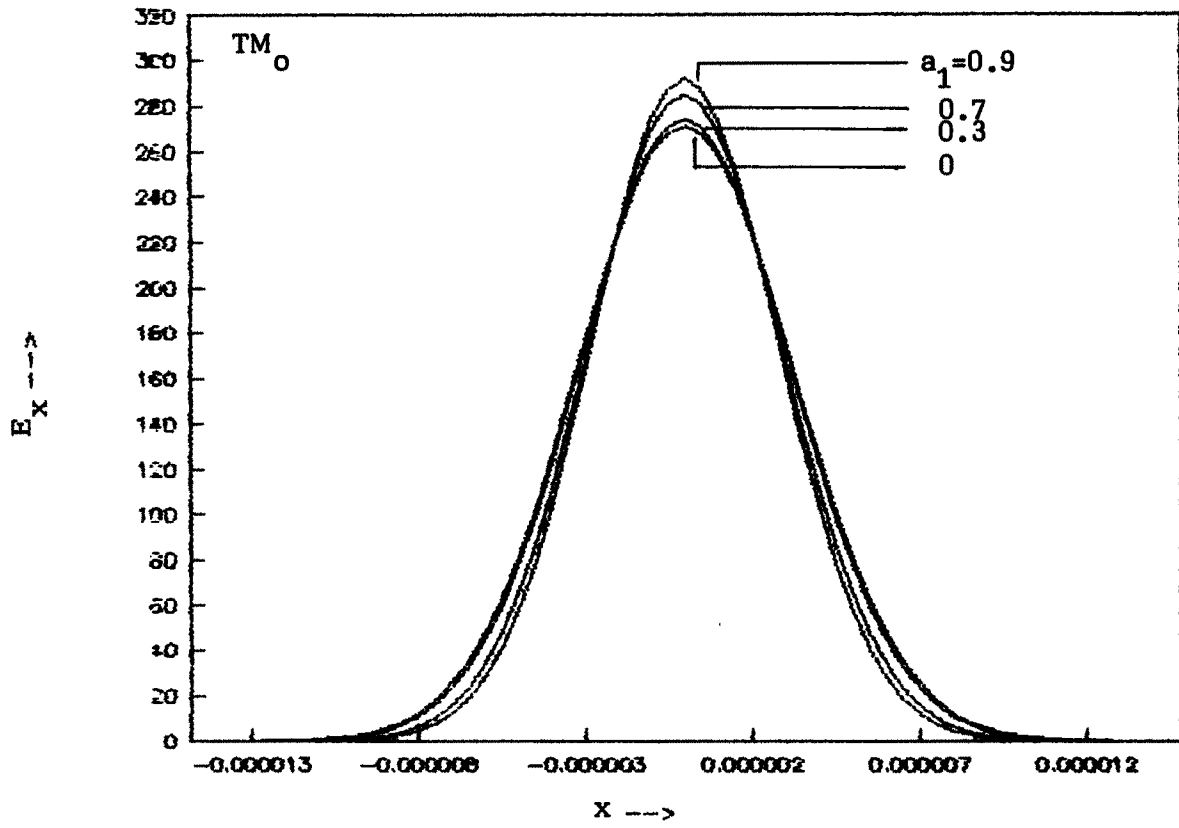
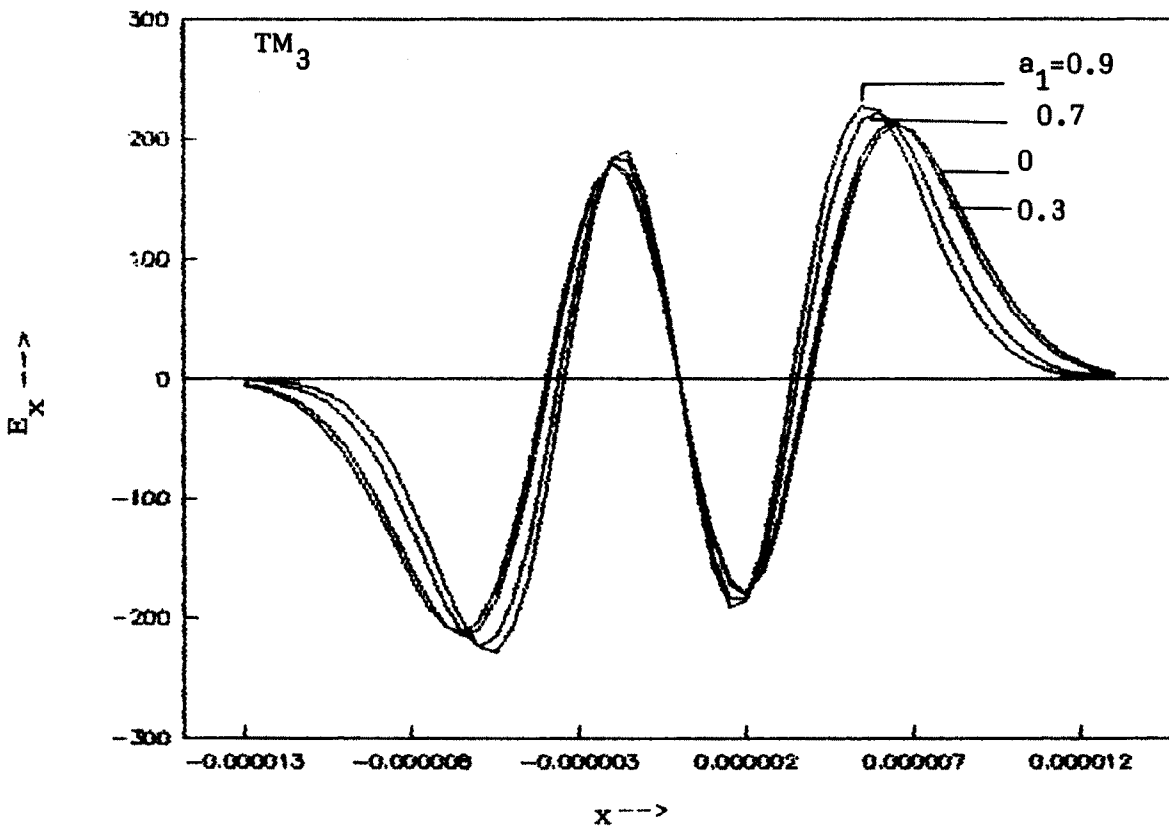
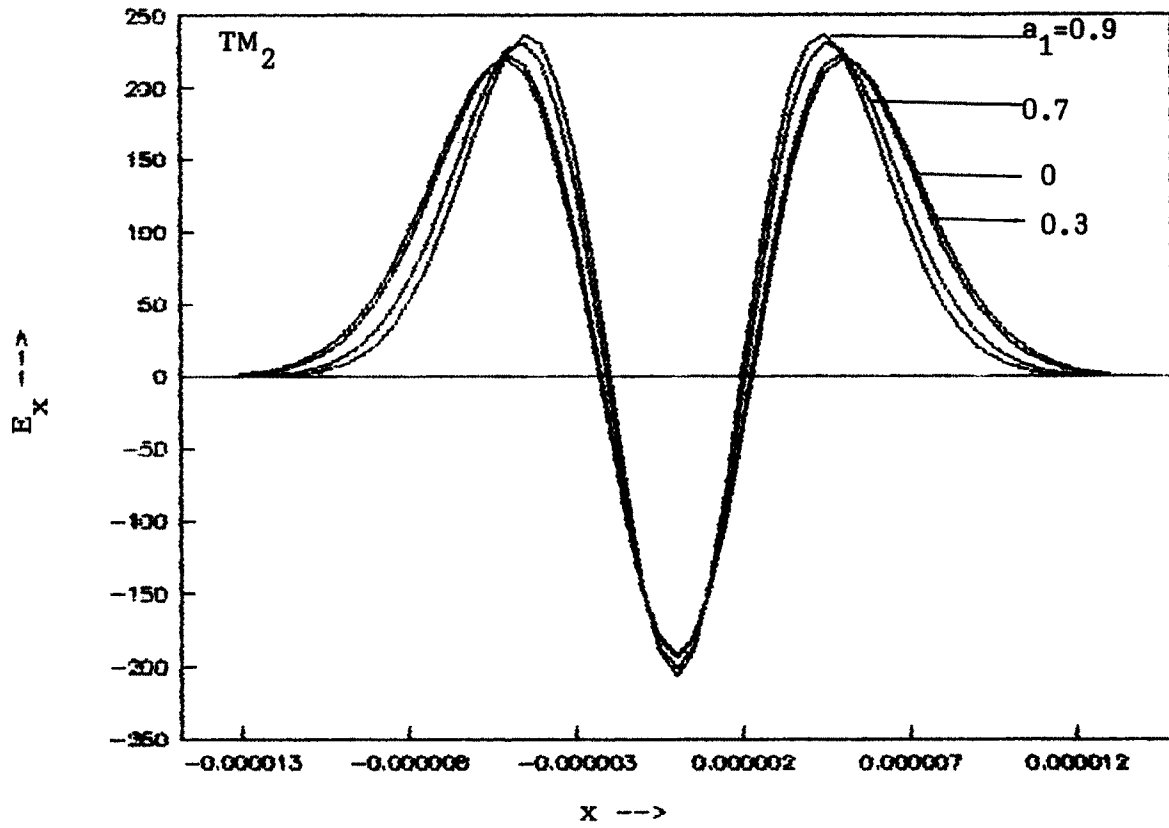
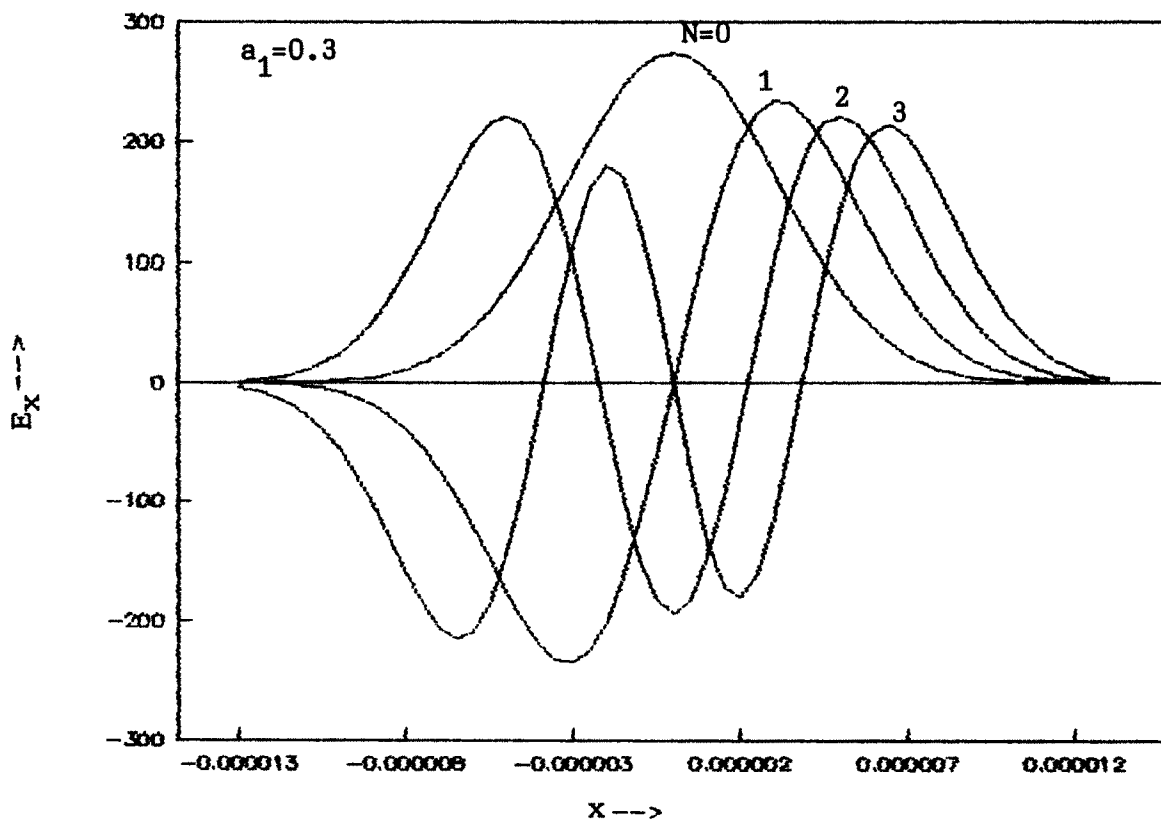
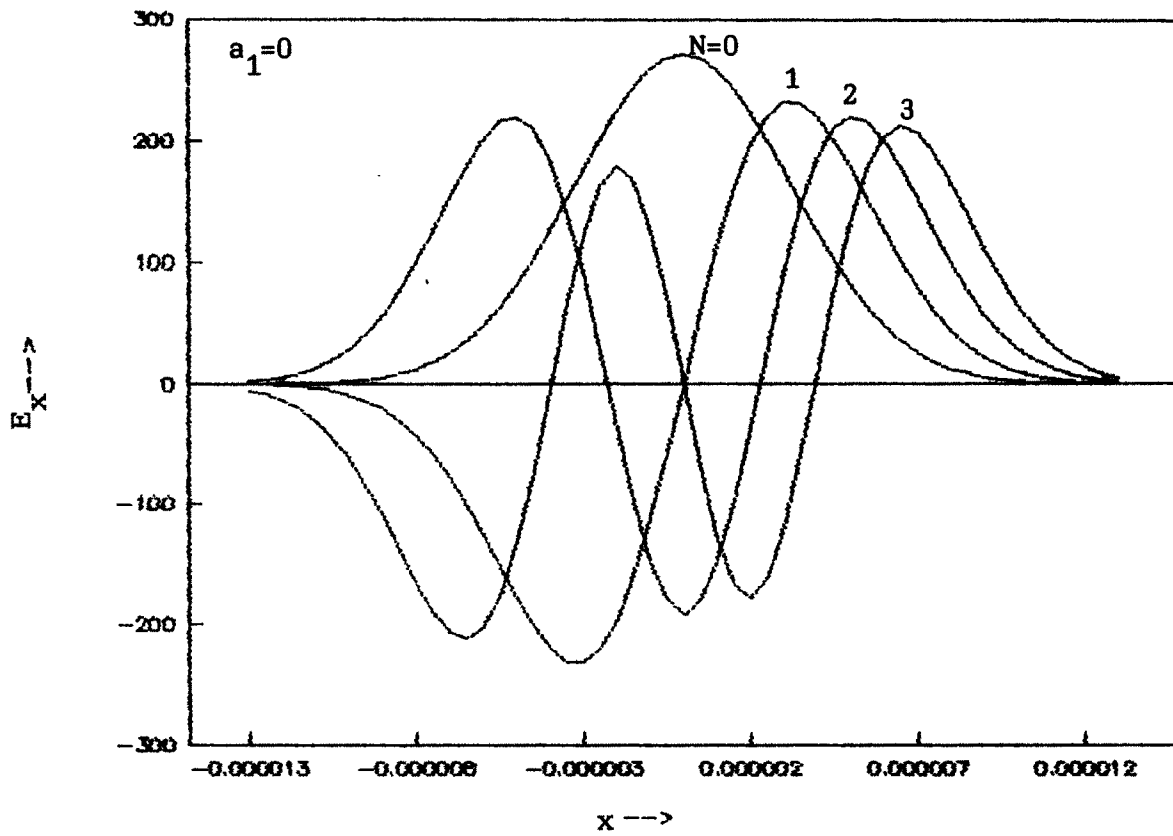


Fig 3.11 : Field distributions for  $TM_2$  and  $TM_3$  modes.



**Fig 3.12** : Comparative Field distributions of TM modes for  $a/\rho = 0$  and  $0.3$  .



**Fig 3.13** : Comparative Field distributions of TM modes for  $a/\rho = 0.7$  and  $0.9$  .

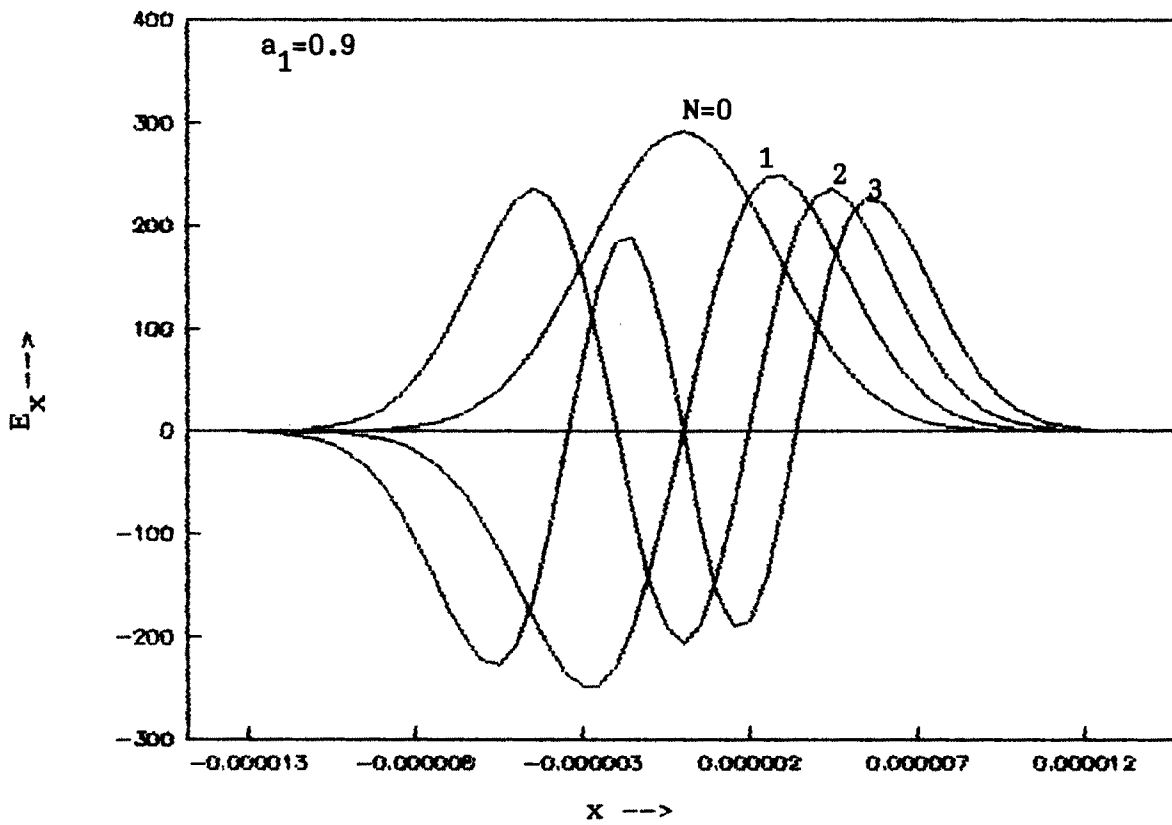
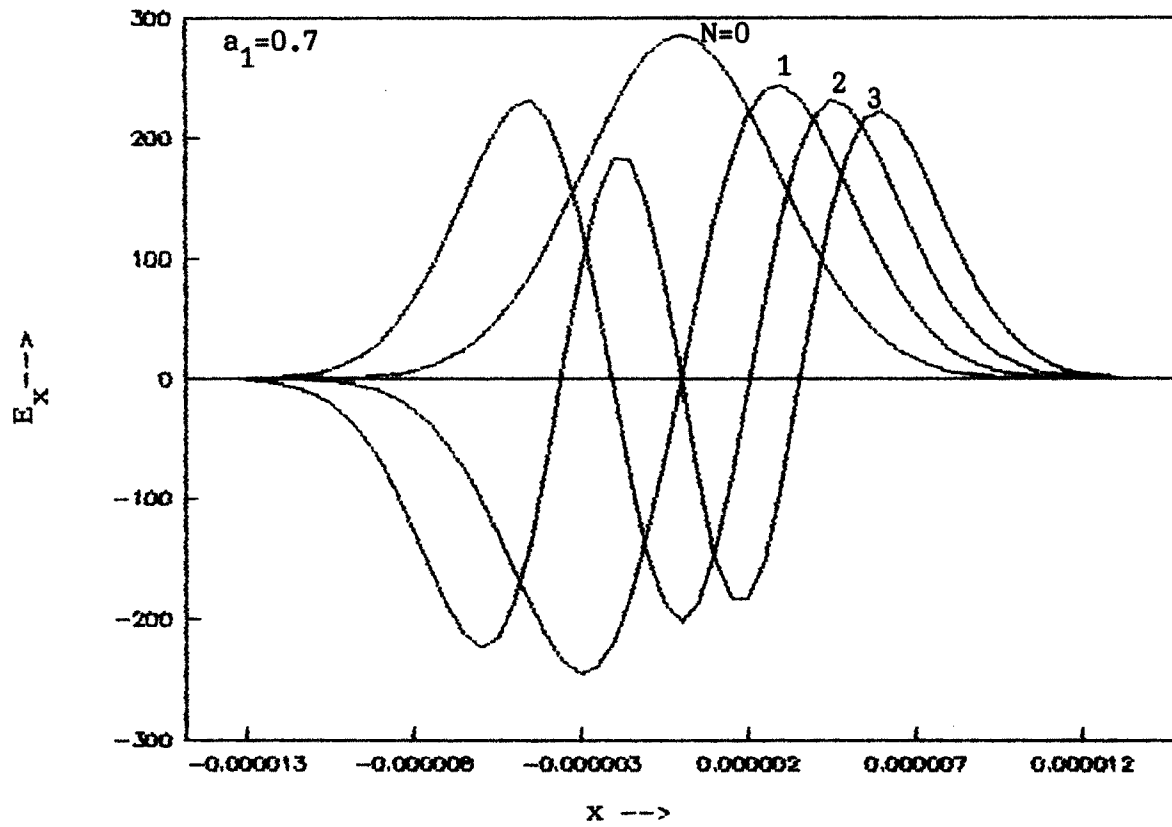


Fig 3.14 :  $\bar{b} - v$  curves for  $TM_0$  and  $TM_1$  modes.

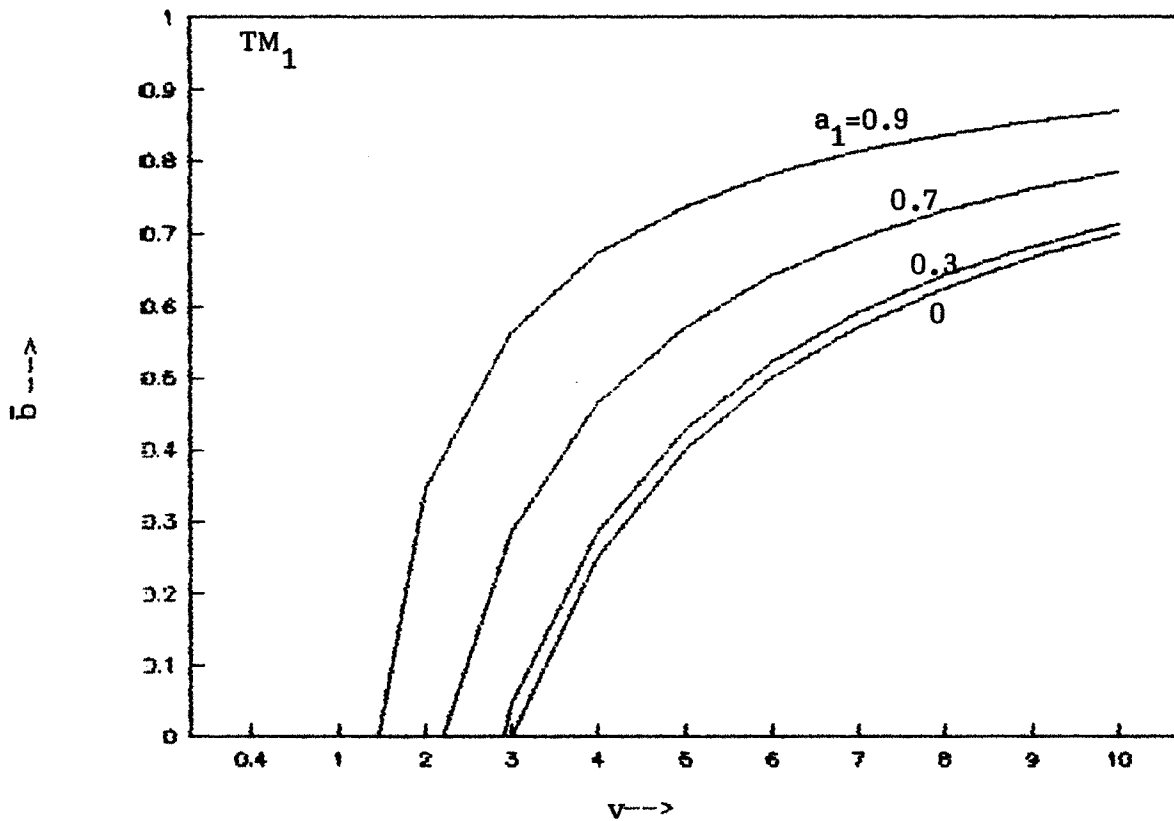
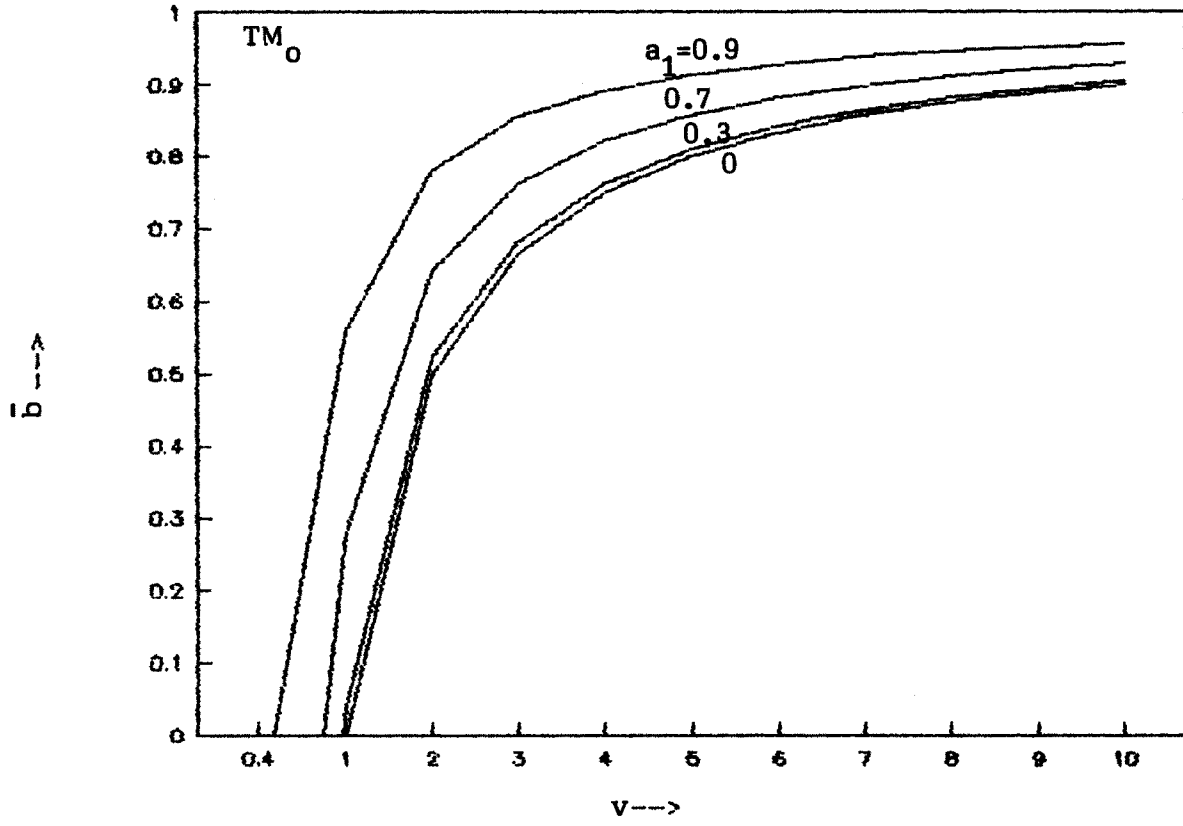


Fig 3.15 :  $\bar{b} - v$  curves for  $TM_2$  and  $TM_3$  modes.

